

Supplementary Figure 1 (related to Figures 1 and 2): Schematic to study the metabolic phenotypes in offspring (F1) obtained from insulin resistant parents (F0). (A) Breeding scheme. In brief, control offspring were derived by breeding a control male and female (insulin receptor $^{lox/lox}$; Albumin-Cre $^{-/-}$). FL offspring were derived by breeding a male LIRKO (insulin receptor $^{lox/lox}$; Albumin-Cre $^{+/-}$) with a control female. ML offspring were derived by breeding a control male with a LIRKO female. (B-C) Blood glucose values following an intraperitoneal glucose tolerance test in control (black) or LIRKO (red) females (B) and control (black) or LIRKO (blue) males (C). Glucose levels plotted as % of basal values, following intraperitoneal injection of insulin in control or LIRKO females (D) and control or LIRKO males (E). (F) Random-fed blood glucose levels in control or LIRKO females. (G) Random-fed blood glucose levels in control or LIRKO males. (H) Random-fed serum insulin levels in control or LIRKO females. (I) Random-fed serum insulin levels in control or LIRKO males. (J) Body weight of controls or LIRKO females at 2 months of age. (K) Body composition in controls and LIRKO females at 2 months of age. (L) Body weight of controls and LIRKO males at 2 months of age. (M) Body composition of controls and LIRKO males at 2 months of age. All data from n=4-9/group and analyzed using the unpaired two-tailed Student's t-test. *P< 0.05, **P< 0.01 and ***P< 0.001. Data are expressed as means \pm SEM.

Supplementary Figure 1 (related to Figure 1 and 2)

Supplementary Table 1: Random-fed serum metabolites from F0 parents

	Control (n=3-4)	LIRKO (n=3-4)
F0 Mothers (ML)		
C-peptide (ng/mL)	2.2 ± 0.8	1.4 ± 0.1
Leptin (ng/mL)	5.6 ± 1.6	3.9 ± 0.6
MCP-1 (pg/mL)	38.2 ± 9.3	10.7 ± 3.2
Resistin (pg/mL)	7353.4 ± 606.4	6214 ± 658.8
F0 Fathers (FL)		
C-peptide (ng/mL)	1.7 ± 0.3	2.4 ± 0.4
Leptin (ng/mL)	8.5 ± 1.5	5.4 ± 1.4
MCP-1 (pg/mL)	307 ± 112.3	14.4 ± 2.1
Resistin (pg/mL)	6318.8 ± 313.2	6701.8 ± 662.6

Supplementary Table 2: Random-fed serum metabolites in male F1 offspring at 3 months of age

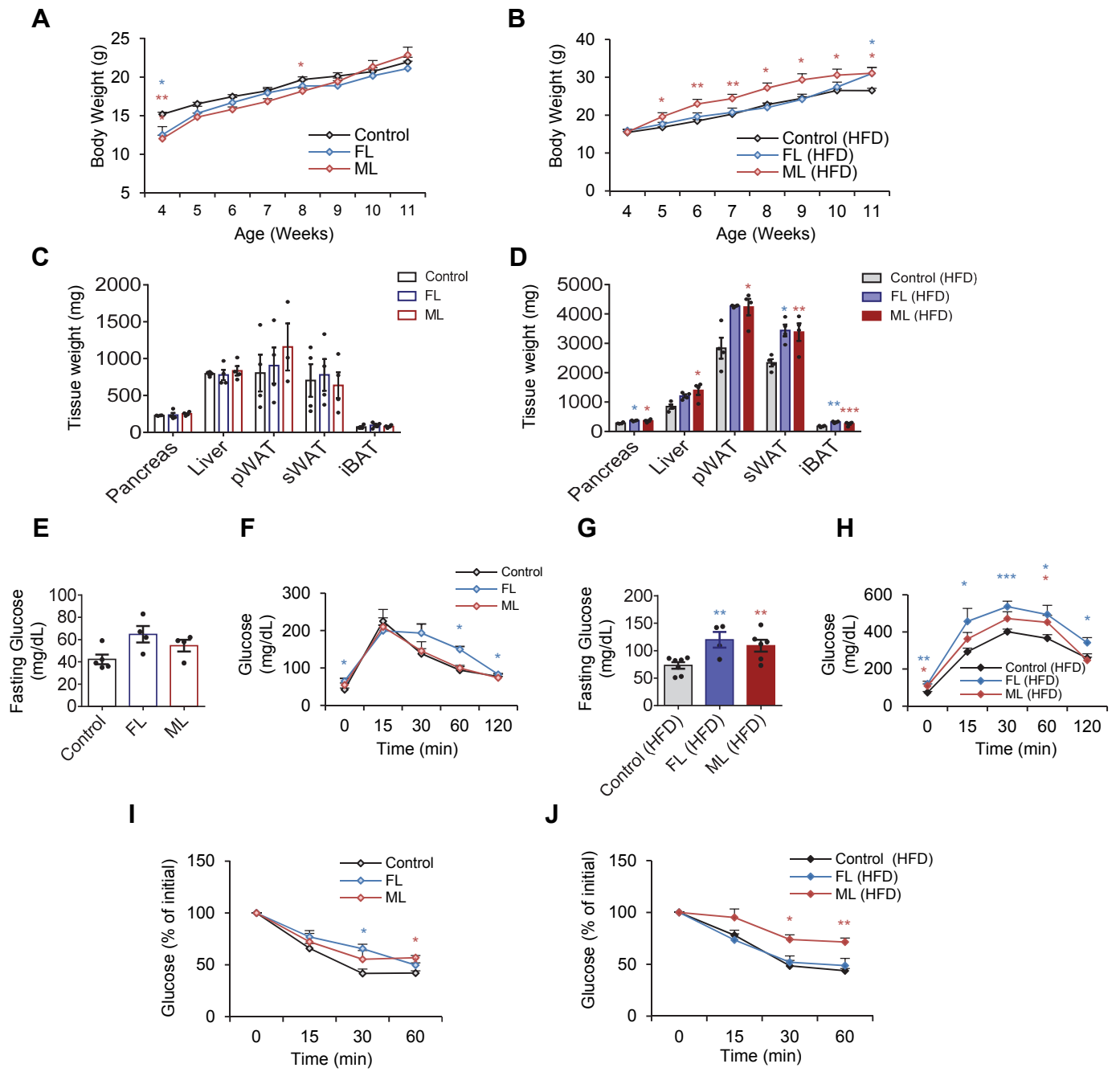
F1 Offspring	Control	FL	ML	Control (HFD)	FL (HFD)	ML (HFD)
Insulin (ng/mL)	5.0 ± 0.4	3.6 ± 1.3	3.5 ± 0.3^a	13 ± 6.3	14.6 ± 4.1	14.9 ± 4.1
C-peptide (ng/mL)	3.2 ± 0.8	1.6 ± 0.5	1.8 ± 0.6	2.7 ± 1.6	2.6 ± 1.4	1.8 ± 0.6
Leptin (ng/mL)	9.6 ± 2.9	5.9 ± 1.7	9.8 ± 3.1	22.9 ± 1.8	33.2 ± 3.7^c	28.8 ± 2.6
GIP (pg/mL)	77.6 ± 34.7	126.9 ± 45.6	76.5 ± 24.7	338.9 ± 179.3	199.1 ± 91.9	131 ± 42
MCP-1 (pg/mL)	16 ± 7.9	57.2 ± 6.4^b	23.7 ± 5.2	203.7 ± 44.8	50 ± 7.1^c	70.9 ± 9.8^d
Resistin (pg/mL)	5224.8 ± 2248.1	5902.5 ± 856.3	3933.8 ± 1168	8411.8 ± 1637.5	5740.2 ± 1444	4914.8 ± 789.4^d

^a p<0.05 (Control Vs. ML)

^b p<0.01 (Control Vs. FL)

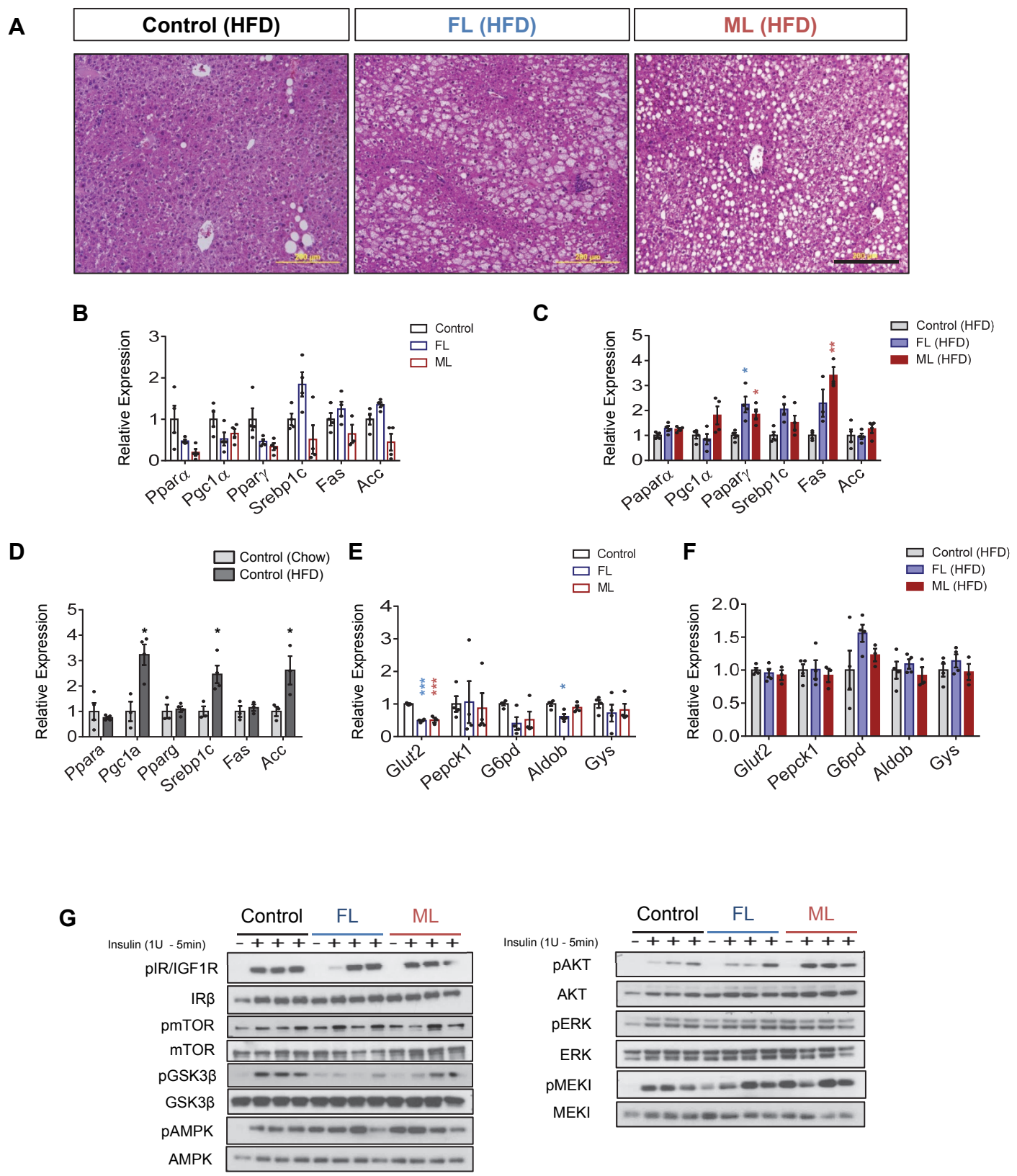
^c p<0.05 (Control HFD Vs. FL HFD)

^d p<0.05 (Control HFD Vs. ML HFD)

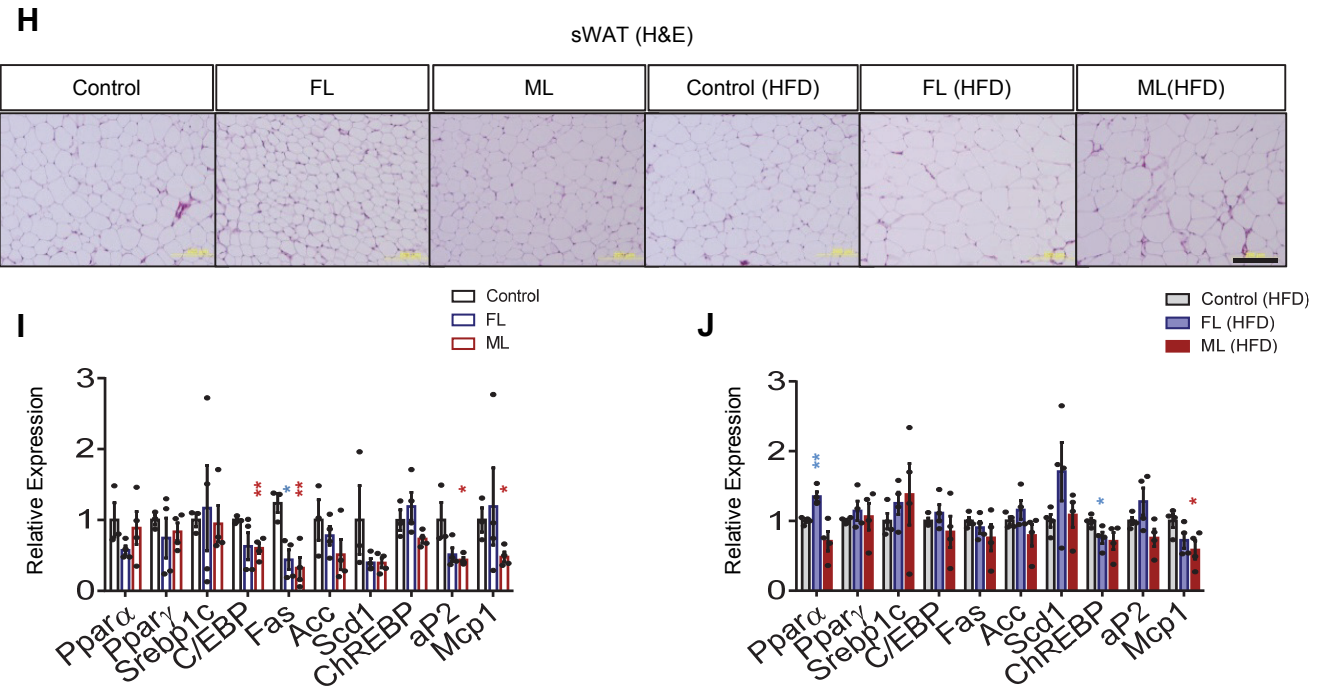


Supplementary Figure 2 (related to figure 1 and 2): Females F1 offspring from insulin resistant parents present metabolic abnormalities similar to male siblings. (A-B) Body weight trajectories in control (black), FL (blue) or ML (red) female offspring on chow (A) or HFD (B) diets. (C-D) Body weight composition in mice on chow (C) or HFD (D) diets at 3 months of age. (E) Fasted blood glucose levels in control, FL or ML offspring on chow diet at 2 months of age. (F) Blood glucose values following an intraperitoneal glucose tolerance test in control, FL, and ML in chow. (G) Fasted blood glucose levels in control, FL or ML on HFD diet at 2 months of age. (H) Blood glucose values following an intraperitoneal glucose tolerance test in control, FL, or ML on HFD diets. (I-J) Insulin tolerance test with glucose levels plotted as % of basal values, following intraperitoneal injection of insulin in control, FL, or ML on chow (I) or HFD (J) diets. All data are based on n=4-8/group representing a minimum of 3 independent litters/group. Statistical analyses by multiple t-tests corrected for multiple comparisons with Holm-Sidak method in “C” and “D”, and one-way ANOVA with Dunnett’s post hoc test in remaining. * P < 0.05, ** P < 0.01 and ***P < 0.001. Data are expressed as means ± SEM. . pWAT- perigonadal white adipose tissue; sWAT- flank subcutaneous white adipose tissue; iBAT- interscapular brown adipose tissue.

Supplementary Figure 2 (related to Figure 1 and 2)

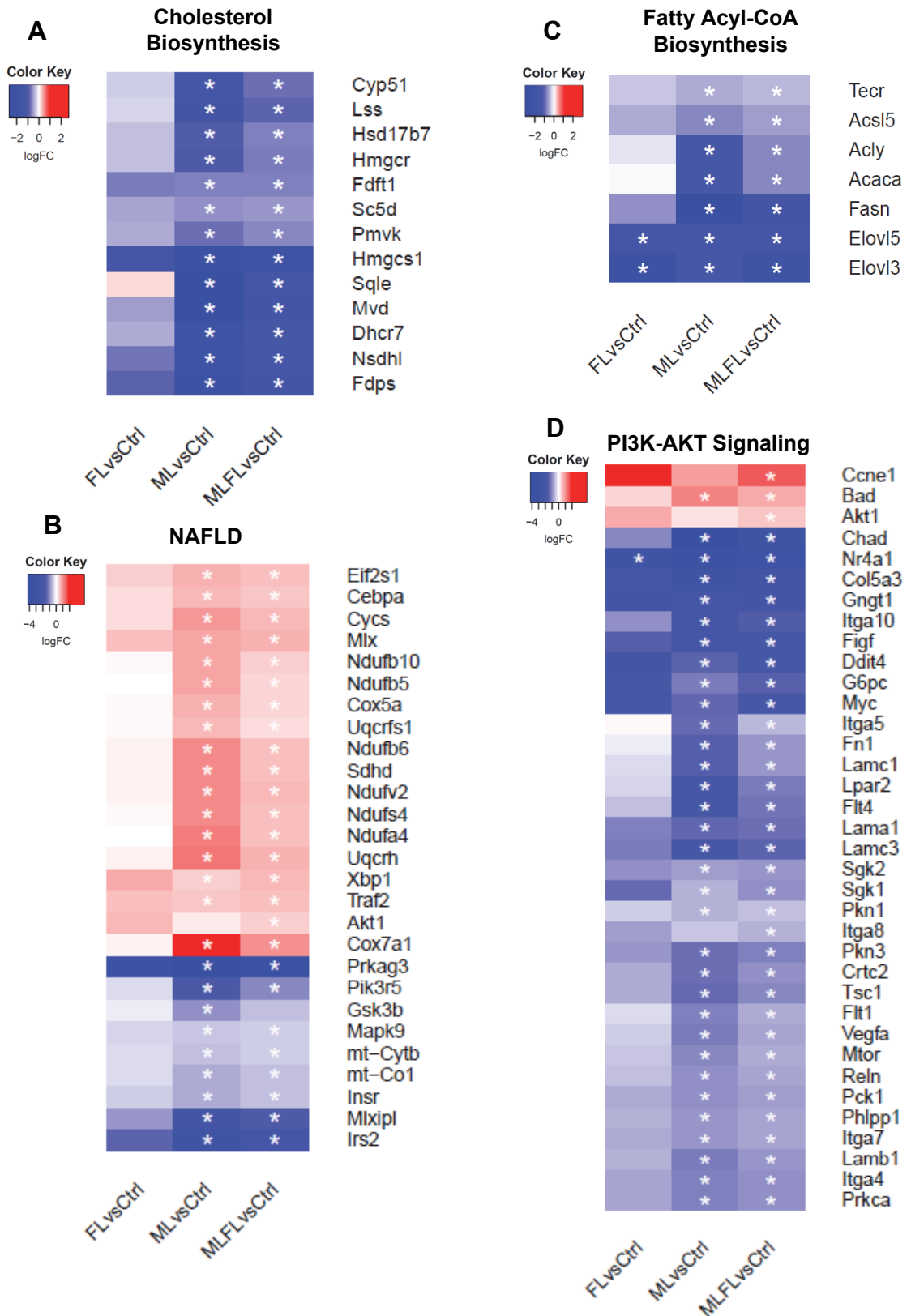


Supplementary Figure 3 (related to Figure 2 and 3)



Supplementary Figure 3 (related to figure 2 and 3): Extended phenotypic characterization in F1 male offspring. (A) High magnification Hematoxylin and Eosin-stained (H and E) liver sections from control, FL or ML offspring (Magnification 200x, scale bar = 200 μ m). (B-C) qPCR analysis of genes involved in lipid β -oxidation and fatty acid synthesis in chow (B) and HFD (C).(D) qPCR comparison of gene expression between control on chow versus HFD diets. (E-F). Further hepatic expression analysis of genes involved in glucose transport, glycolysis, gluconeogenesis and glycogenesis on chow (E) or HFD (F) diets. (G) Signaling analysis in liver lysates from control, FL or ML offspring in chow following vena-cava infusion of insulin. (H) Representative H and E stained flank subcutaneous white adipose tissue (sWAT) sections in control, FL or ML on chow or HFD diets (Magnification 200x, scale bar = 200 μ m). (I-J) qPCR analyses of genes involved in lipid biology and inflammation on chow (I) or (J) HFD diets. All data are based on n=3-9/group representing a minimum of 3 independent litters/group. Statistical analyses by multiple t-tests corrected for multiple comparisons with Holm-Sidak method. *P< 0.05, **P< 0.01 and ***P< 0.001. Data are expressed as means \pm SEM.

Supplementary Figure 3 (Cont.)



Supplementary Figure 4 (related to figure 2 and 3): (A-D) Heat-map representation of differently expressed genes related to cholesterol biosynthesis (A), NAFLD (B), fatty Acyl-CoA biosynthesis (C), and PI3K-AKT signaling (D) in FL and ML offspring compared to controls. *represent FDR<0.10.

Supplementary Figure 4 (related to Figure 3)

Supplementary Table 3: Enriched Pathway Analyses – RNA-Seq. FL/ML vs. Controls (Genes with FDR<0.25) (1/3)

pathway name	set size	candidates	p-value	pathway source
Gene Expression	720	275 (38.2%)	5.79E-40	Reactome
Translation	200	115 (57.5%)	2.98E-36	Reactome
SRP-dependent cotranslational protein targeting to membrane	160	100 (62.5%)	5.39E-36	Reactome
Ribosome - Mus musculus (mouse)	161	99 (62.7%)	8.82E-36	KEGG
Eukaryotic Translation Elongation	135	88 (65.2%)	7.36E-34	Reactome
Formation of a pool of free 40S subunits	143	91 (63.6%)	9.58E-34	Reactome
Peptide chain elongation	132	86 (65.2%)	4.35E-33	Reactome
GTP hydrolysis and joining of the 60S ribosomal subunit	156	95 (60.9%)	6.51E-33	Reactome
L13a-mediated translational silencing of Ceruloplasmin expression	154	94 (61.0%)	1.08E-32	Reactome
3'-UTR-mediated translational regulation	154	94 (61.0%)	1.08E-32	Reactome
Cap-dependent Translation Initiation	163	97 (59.5%)	2.06E-32	Reactome
Eukaryotic Translation Initiation	163	97 (59.5%)	2.06E-32	Reactome
Eukaryotic Translation Termination	132	85 (64.4%)	3.76E-32	Reactome
Metabolism of mRNA	215	114 (53.0%)	1.70E-31	Reactome
Nonsense Mediated Decay Independent of the Exon Junction Complex	137	86 (62.8%)	2.68E-31	Reactome
Metabolism of RNA	264	128 (48.5%)	3.40E-30	Reactome
Nonsense Mediated Decay Enhanced by the Exon Junction Complex	147	88 (59.9%)	9.03E-30	Reactome
Nonsense-Mediated Decay	147	88 (59.9%)	9.03E-30	Reactome
Cytoplasmic Ribosomal Proteins	79	54 (68.4%)	9.85E-23	WikiPathways
Formation of the ternary complex, and subsequently, the 43S complex	63	45 (71.4%)	2.24E-20	Reactome
Activation of the mRNA upon binding of the cap-binding complex and eIFs, and subsequent binding to 43S	71	48 (67.6%)	4.94E-20	Reactome
Translation initiation complex formation	70	47 (67.1%)	1.88E-19	Reactome
Ribosomal scanning and start codon recognition	71	47 (66.2%)	4.60E-19	Reactome
Metabolism of proteins	521	176 (33.8%)	1.03E-18	Reactome
mRNA processing	465	137 (30.7%)	2.83E-11	WikiPathways
Cholesterol Biosynthesis	15	13 (86.7%)	1.60E-08	WikiPathways
G2/M Transition	103	43 (41.7%)	1.80E-08	Reactome
Mitotic G2-G2/M phases	105	43 (41.0%)	3.56E-08	Reactome
Regulation of PLK1 Activity at G2/M Transition	79	35 (44.3%)	6.35E-08	Reactome
mRNA Splicing - Major Pathway	112	44 (39.3%)	1.06E-07	Reactome
mRNA Splicing	112	44 (39.3%)	1.06E-07	Reactome
Transcription	180	61 (33.9%)	2.44E-07	Reactome
Transcriptional Regulation of Adipocyte Differentiation in 3T3-L1 Pre-adipocytes	42	22 (52.4%)	5.21E-07	Reactome
Transcriptional Regulation of White Adipocyte Differentiation	42	22 (52.4%)	5.21E-07	Reactome
Centrosome maturation	68	30 (44.1%)	6.15E-07	Reactome
Recruitment of mitotic centrosome proteins and complexes	68	30 (44.1%)	6.15E-07	Reactome
Dual incision reaction in TC-NER	28	17 (60.7%)	6.43E-07	Reactome
Formation of transcription-coupled NER (TC-NER) repair complex	28	17 (60.7%)	6.43E-07	Reactome
Focal Adhesion	182	60 (33.0%)	8.84E-07	WikiPathways
mRNA Processing	163	55 (33.7%)	1.10E-06	Reactome
Processing of Capped Intron-Containing Pre-mRNA	144	50 (34.7%)	1.30E-06	Reactome
Focal adhesion - Mus musculus (mouse)	206	65 (31.6%)	1.79E-06	KEGG
Cholesterol biosynthesis	22	14 (63.6%)	2.91E-06	Reactome
superpathway of cholesterol biosynthesis	25	15 (60.0%)	3.69E-06	MouseCyc
mRNA Capping	28	16 (57.1%)	4.25E-06	Reactome
Loss of proteins required for interphase microtubule organization from the centrosome	60	26 (43.3%)	5.14E-06	Reactome
Loss of Nip from mitotic centrosomes	60	26 (43.3%)	5.14E-06	Reactome
XPodNet - protein-protein interactions in the podocyte expanded by STRING	831	199 (24.0%)	5.53E-06	WikiPathways
RNA Pol II CTD phosphorylation and interaction with CE	26	15 (57.7%)	7.26E-06	Reactome
RNA polymerase - Mus musculus (mouse)	29	16 (55.2%)	7.88E-06	KEGG
cholesterol biosynthesis III (via desmosterol)	11	9 (81.8%)	8.00E-06	MouseCyc
Formation of the Early Elongation Complex	32	17 (53.1%)	8.10E-06	Reactome
ECM-receptor interaction - Mus musculus (mouse)	87	33 (37.9%)	9.86E-06	KEGG
Developmental Biology	307	86 (28.0%)	1.01E-05	Reactome
Laminin interactions	21	13 (61.9%)	1.04E-05	Reactome
estrogen signalling	74	29 (39.2%)	1.63E-05	WikiPathways
mRNA Splicing - Minor Pathway	43	20 (46.5%)	1.76E-05	Reactome
RNA Polymerase I, RNA Polymerase III, and Mitochondrial Transcription	90	33 (36.7%)	2.25E-05	Reactome
cholesterol biosynthesis I	12	9 (75.0%)	2.68E-05	MouseCyc
Huntington's disease - Mus musculus (mouse)	189	57 (30.2%)	3.35E-05	KEGG
Protein export - Mus musculus (mouse)	30	15 (51.7%)	4.21E-05	KEGG
cholesterol biosynthesis II (via 24,25-dihydrolanosterol)	8	7 (87.5%)	4.28E-05	MouseCyc
Formation of RNA Pol II elongation complex	42	19 (45.2%)	4.61E-05	Reactome
RNA Polymerase II Transcription Elongation	42	19 (45.2%)	4.61E-05	Reactome
RNA Polymerase II Transcription	105	36 (34.3%)	5.20E-05	Reactome
NOTCH1 Intracellular Domain Regulates Transcription	39	18 (46.2%)	5.25E-05	Reactome
Metabolism	1386	303 (21.9%)	7.62E-05	Reactome

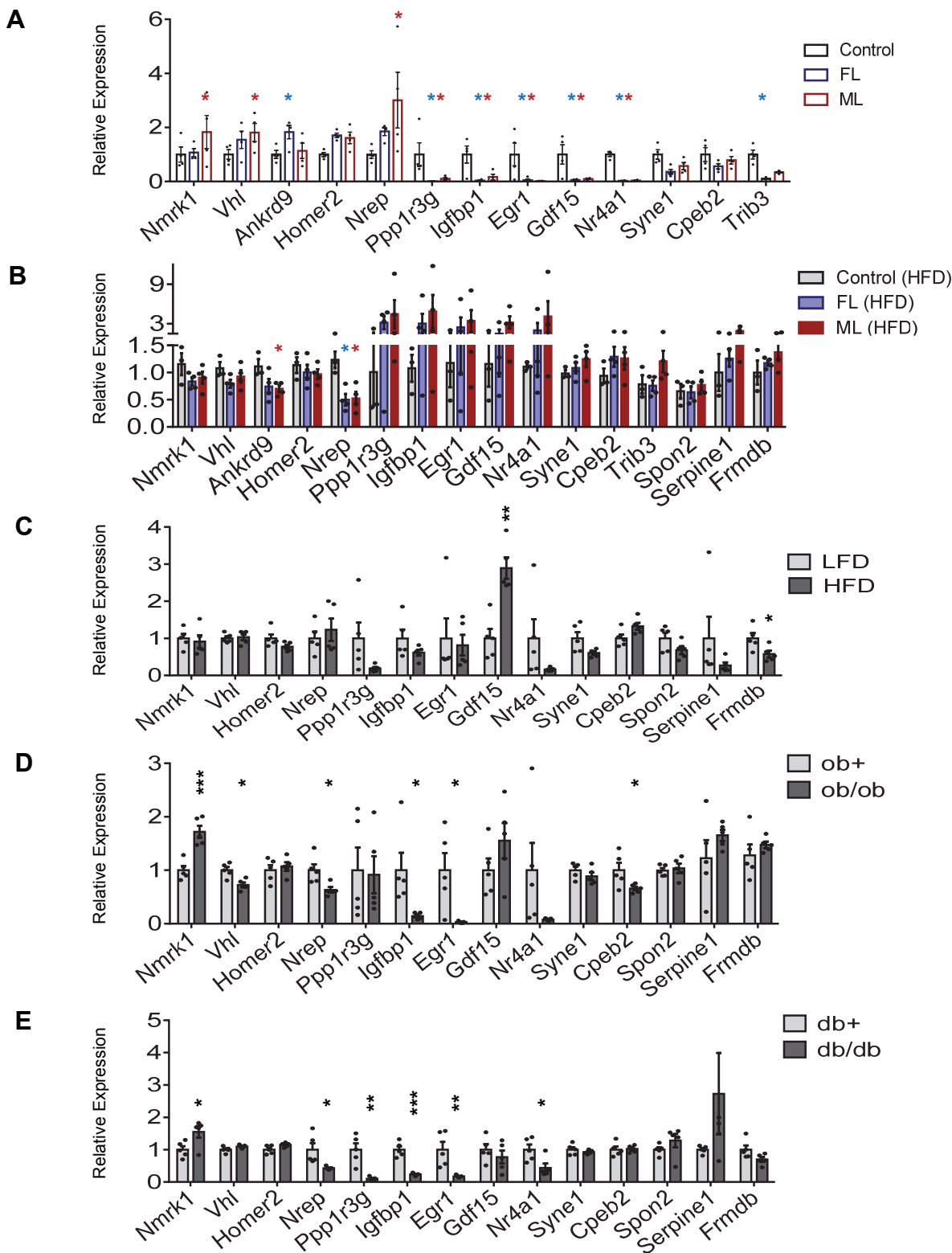
Supplementary Table 3: Enriched Pathway Analyses – RNA-Seq. FL/ML vs. Controls (Genes with FDR<0.25) (2/3)

Purine metabolism	169	51 (30.2%)	8.37E-05	WikiPathways
RNA Polymerase I Promoter Clearance	48	20 (41.7%)	0.000122	Reactome
RNA Polymerase II Promoter Escape	38	17 (44.7%)	0.000137	Reactome
Rho GTPase cycle	118	38 (32.2%)	0.00015	Reactome
Signaling by Rho GTPases	118	38 (32.2%)	0.00015	Reactome
Regulation of mRNA Stability by Proteins that Bind AU-rich Elements	35	16 (45.7%)	0.000157	Reactome
Oxidative Stress Induced Senescence	71	26 (36.6%)	0.000166	Reactome
Packaging Of Telomere Ends	14	9 (64.3%)	0.000172	Reactome
Cellular responses to stress	127	40 (31.5%)	0.000174	Reactome
Purine metabolism - Mus musculus (mouse)	174	51 (29.3%)	0.000188	KEGG
RNA Polymerase II Transcription Pre-Initiation And Promoter Opening	39	17 (43.6%)	0.000202	Reactome
RNA Polymerase II Transcription Initiation	39	17 (43.6%)	0.000202	Reactome
RNA Polymerase II Transcription Initiation And Promoter Clearance	39	17 (43.6%)	0.000202	Reactome
Post-transcriptional Silencing By Small RNAs	7	6 (85.7%)	0.000208	Reactome
Disease	608	144 (23.7%)	0.000225	Reactome
TNF-alpha NF-κB Signaling Pathway	184	53 (28.8%)	0.000231	WikiPathways
RNA Polymerase I Transcription	50	20 (40.0%)	0.000237	Reactome
RNA Polymerase II Pre-transcription Events	58	22 (37.9%)	0.00029	Reactome
RNA Polymerase I Chain Elongation	40	17 (42.5%)	0.000292	Reactome
Spliceosome - Mus musculus (mouse)	137	41 (30.4%)	0.000345	KEGG
Transcription-coupled NER (TC-NER)	44	18 (40.9%)	0.000346	Reactome
Cellular Senescence	111	35 (31.5%)	0.000421	Reactome
Elongation arrest and recovery	31	14 (45.2%)	0.000471	Reactome
Semaphorin interactions	64	23 (35.9%)	0.00053	Reactome
Nucleotide Excision Repair	49	19 (38.8%)	0.000537	Reactome
Non-alcoholic fatty liver disease (NAFLD) - Mus musculus (mouse)	160	46 (28.8%)	0.000607	KEGG
RNA Polymerase III Abortive And Retractive Initiation	39	16 (41.0%)	0.000704	Reactome
RNA Polymerase III Transcription	39	16 (41.0%)	0.000704	Reactome
Signaling by NOTCH	81	27 (33.3%)	0.000715	Reactome
Eukaryotic Transcription Initiation	40	16 (40.0%)	0.000978	WikiPathways
Ubiquitin mediated proteolysis - Mus musculus (mouse)	143	41 (28.9%)	0.00107	KEGG
Synthesis of bile acids and bile salts via 27-hydroxycholesterol	14	8 (57.1%)	0.00122	Reactome
RNA Polymerase III Transcription Initiation	34	14 (41.2%)	0.00144	Reactome
Metabolism of lipids and lipoproteins	491	115 (23.4%)	0.00144	Reactome
Lysine degradation - Mus musculus (mouse)	49	18 (36.7%)	0.00156	KEGG
aerobic respiration – electron donor II	86	27 (31.8%)	0.00162	MouseCyc
PodNet: protein-protein interactions in the podocyte	315	78 (24.8%)	0.0017	WikiPathways
ABC-family proteins mediated transport	31	13 (41.9%)	0.00173	Reactome
Circadian rhythm - Mus musculus (mouse)	31	13 (41.9%)	0.00173	KEGG
DNA Repair	107	32 (29.9%)	0.00194	Reactome
RNA Polymerase III Transcription Initiation From Type 3 Promoter	28	12 (42.9%)	0.00207	Reactome
Respiratory electron transport	74	24 (32.4%)	0.00211	Reactome
Signaling by NOTCH1	62	21 (33.9%)	0.00215	Reactome
Signaling by NOTCH1 t(7;9)(NOTCH1:M1580_K2555) Translocation Mutant	62	21 (33.9%)	0.00215	Reactome
Signaling by NOTCH1 HD Domain Mutants in Cancer	62	21 (33.9%)	0.00215	Reactome
Signaling by NOTCH1 PEST Domain Mutants in Cancer	62	21 (33.9%)	0.00215	Reactome
Signaling by NOTCH1 HD+PEST Domain Mutants in Cancer	62	21 (33.9%)	0.00215	Reactome
FBXW7 Mutants and NOTCH1 in Cancer	62	21 (33.9%)	0.00215	Reactome
Signaling by NOTCH1 in Cancer	62	21 (33.9%)	0.00215	Reactome
Axon guidance	225	58 (25.8%)	0.00244	Reactome
RNA Polymerase I Transcription Initiation	25	11 (44.0%)	0.00246	Reactome
Insulin Signaling	157	43 (27.4%)	0.00254	WikiPathways
RNA transport - Mus musculus (mouse)	172	46 (26.9%)	0.00271	KEGG
Bile acid and bile salt metabolism	36	14 (38.9%)	0.00274	Reactome
Delta-Notch Signaling Pathway	84	26 (31.0%)	0.00294	WikiPathways
Electron Transport Chain	102	30 (29.7%)	0.00297	WikiPathways
Cell Cycle	408	96 (23.5%)	0.00298	Reactome
Non-integrin membrane-ECM interactions	33	13 (39.4%)	0.00337	Reactome
CRMPs in Sema3A signaling	16	8 (50.0%)	0.00369	Reactome
Circadian Clock	13	7 (53.8%)	0.00392	Reactome
Circadian Clock	13	7 (53.8%)	0.00392	Reactome
Protein folding	45	16 (35.6%)	0.00407	Reactome
RNA Polymerase III Transcription Termination	23	10 (43.5%)	0.00428	Reactome
Cyclin E associated events during G1/S transition	23	10 (43.5%)	0.00428	Reactome
Cyclin A:Cdk2-associated events at S phase entry	23	10 (43.5%)	0.00428	Reactome
Synthesis of bile acids and bile salts via 7alpha-hydroxycholesterol	23	10 (43.5%)	0.00428	Reactome
Meiotic Recombination	23	10 (43.5%)	0.00428	Reactome
Amyloids	23	10 (43.5%)	0.00428	Reactome
IL-6 signaling Pathway	99	29 (29.3%)	0.0043	WikiPathways
EGFR1 Signaling Pathway	176	46 (26.3%)	0.00438	WikiPathways
Histidine catabolism	5	4 (80.0%)	0.0046	Reactome
Extracellular matrix organization	227	57 (25.1%)	0.00487	Reactome
Synthesis of bile acids and bile salts	27	11 (40.7%)	0.00506	Reactome

Supplementary Table 3: Enriched Pathway Analyses – RNA-Seq. FL/ML vs. Controls (Genes with FDR<0.25) (3/3)

ErbB signaling pathway	46	16 (34.8%)	0.00521	Wikipathways
Collagen biosynthesis and modifying enzymes	54	18 (33.3%)	0.00525	Reactome
Starch and sucrose metabolism - <i>Mus musculus</i> (mouse)	54	18 (33.3%)	0.00525	KEGG
Respiratory electron transport, ATP synthesis by chemiosmotic coupling, and heat production by uncoupling proteins.	92	27 (29.3%)	0.00559	Reactome
PI3K-Akt signaling pathway - <i>Mus musculus</i> (mouse)	356	83 (23.5%)	0.00562	KEGG
Generic Transcription Pathway	123	34 (27.6%)	0.00581	Reactome
Steroid biosynthesis - <i>Mus musculus</i> (mouse)	17	8 (47.1%)	0.00588	KEGG
Pre-NOTCH Expression and Processing	17	8 (47.1%)	0.00588	Reactome
Fatty Acyl-CoA Biosynthesis	17	8 (47.1%)	0.00588	Reactome
SEMA3A-Plexin repulsion signaling by inhibiting Integrin adhesion	14	7 (50.0%)	0.00662	Reactome
SREBF and miR33 in cholesterol and lipid homeostasis	14	7 (50.0%)	0.00662	Wikipathways
Oxidative phosphorylation - <i>Mus musculus</i> (mouse)	142	38 (26.8%)	0.00662	KEGG
Fc gamma R-mediated phagocytosis - <i>Mus musculus</i> (mouse)	89	26 (29.2%)	0.0069	KEGG
Notch-HLH transcription pathway	11	6 (54.5%)	0.00705	Reactome
NICD traffics to nucleus	11	6 (54.5%)	0.00705	Reactome
Peroxisome - <i>Mus musculus</i> (mouse)	81	24 (29.6%)	0.00764	KEGG
Triglyceride Biosynthesis	36	13 (36.1%)	0.00797	Reactome
Integration of energy metabolism	90	26 (28.9%)	0.00807	Reactome
Regulation of Insulin Secretion by Glucagon-like Peptide-1	40	14 (35.0%)	0.00819	Reactome
IL-7 Signaling Pathway	44	15 (34.1%)	0.00828	Wikipathways
Small cell lung cancer - <i>Mus musculus</i> (mouse)	86	25 (29.1%)	0.00852	KEGG
RNA Polymerase III Chain Elongation	18	8 (44.4%)	0.00892	Reactome
G Protein Signaling Pathways	91	26 (28.6%)	0.0094	Wikipathways
Drug metabolism - other enzymes - <i>Mus musculus</i> (mouse)	61	19 (31.1%)	0.00946	KEGG
IL-3 Signaling Pathway	100	28 (28.0%)	0.00966	Wikipathways

Supplementary Figure 5 (related to Figure 3)



Supplementary Figure 5 (related to figure 3). (A) qPCR analyses of selected-candidate genes in FL or ML on chow diet. (B) qPCR analyses of selected-candidate genes in FL or ML on HFD. (C) qPCR analyses of candidate genes on a 6-week low-fat –LFD (white bars) versus HFD diets (black bars). (D) qPCR analyses of candidate genes in leptin-deficient ob/ob mice (black bars) versus ob+ (white bars). (E) qPCR analyses of candidate genes in leptin receptor-deficient db/db mice (black bars) versus db+ (white bars). qPCR in FL, ML and control (n=4 mice/litters). qPCR in other models (n=5 mice). All data are expressed as mean \pm SEM and analyzed using an unpaired two-tailed Student's t-test. * P<0.05, ** P<0.01 and ***P< 0.001.

Supplementary Table 4: Enriched Pathway Analyses – Increased Promoter Methylation (FL/ML vs. Controls) (1/4)

Increased Promoter Methylation (Me.>0%; FDR<5%)	set size	candidates	p-value	pathway source
		contained		
XPodNet - protein-protein interactions in the podocyte expanded by STRING	831	280 (33.9%)	1.25E-13	Wikipathways
PluriNetWork	291	114 (39.3%)	2.74E-10	Wikipathways
PodNet- protein-protein interactions in the podocyte	315	115 (36.5%)	3.42E-08	Wikipathways
Developmental Biology	307	112 (36.6%)	4.42E-08	Reactome
Regulation of Insulin Secretion	69	35 (52.2%)	1.94E-07	Reactome
Integration of energy metabolism	90	42 (47.7%)	3.24E-07	Reactome
Insulin secretion - Mus musculus (mouse)	88	40 (46.0%)	2.05E-06	KEGG
IL-3 Signaling Pathway	100	44 (44.0%)	2.80E-06	Wikipathways
Signalling by NGF	275	95 (34.7%)	6.99E-06	Reactome
EGFR1 Signaling Pathway	176	66 (37.5%)	1.03E-05	Wikipathways
Axon guidance	225	80 (35.7%)	1.07E-05	Reactome
Signaling by FGFR in disease	155	59 (38.3%)	1.42E-05	Reactome
MAPK signaling pathway - Mus musculus (mouse)	257	86 (33.9%)	5.08E-05	KEGG
Pathways in cancer - Mus musculus (mouse)	326	105 (32.5%)	5.42E-05	KEGG
Integrin-mediated Cell Adhesion	98	40 (40.8%)	6.50E-05	Wikipathways
Oocyte meiosis - Mus musculus (mouse)	113	44 (39.6%)	6.62E-05	KEGG
Dopaminergic synapse - Mus musculus (mouse)	135	50 (38.2%)	6.98E-05	KEGG
NGF signalling via TRKA from the plasma membrane	184	65 (35.5%)	8.44E-05	Reactome
Disease	608	179 (29.6%)	8.46E-05	Reactome
Vasopressin-regulated water reabsorption - Mus musculus (mouse)	44	22 (50.0%)	8.64E-05	KEGG
Ubiquitin mediated proteolysis - Mus musculus (mouse)	143	52 (37.4%)	9.32E-05	KEGG
Progesterone-mediated oocyte maturation - Mus musculus (mouse)	89	36 (41.4%)	0.000106	KEGG
mRNA processing	465	138 (30.6%)	0.000107	Wikipathways
Regulation of actin cytoskeleton - Mus musculus (mouse)	218	74 (34.3%)	0.000109	KEGG
T Cell Receptor Signaling Pathway	133	50 (37.6%)	0.000109	Wikipathways
Neurotrophin signalling pathway - Mus musculus (mouse)	123	47 (38.2%)	0.000111	KEGG
Calcium Regulation in the Cardiac Cell	150	55 (36.7%)	0.000111	Wikipathways
Neuronal System	254	84 (33.3%)	0.000114	Reactome
Ras signaling pathway - Mus musculus (mouse)	230	77 (33.9%)	0.000115	KEGG
Cell Cycle, Mitotic	337	107 (31.8%)	0.000133	Reactome
Signaling by SCF-KIT	125	47 (37.9%)	0.000138	Reactome
Fc gamma R-mediated phagocytosis - Mus musculus (mouse)	89	36 (40.9%)	0.00014	KEGG
Regulation of Cholesterol Biosynthesis by SREBP (SREBF)	12	9 (75.0%)	0.000203	Reactome
Hedgehog signaling pathway - Mus musculus (mouse)	49	23 (46.9%)	0.000204	KEGG
Downstream signal transduction	142	51 (36.2%)	0.000285	Reactome
Signaling by PDGF	160	56 (35.2%)	0.000325	Reactome
GABAergic synapse - Mus musculus (mouse)	90	35 (39.8%)	0.00033	KEGG
Wnt Signaling Pathway NetPath	109	41 (38.0%)	0.000346	Wikipathways
Metabolism	1386	366 (26.8%)	0.000374	Reactome
Platelet Aggregation (Plug Formation)	36	18 (50.0%)	0.000377	Reactome
Signaling by EGFR	161	56 (35.0%)	0.000389	Reactome
Wnt Signaling Pathway	60	26 (43.3%)	0.000396	Wikipathways
Signaling by FGFR1 fusion mutants	15	10 (66.7%)	0.000397	Reactome
Signaling by FGFR	144	51 (35.7%)	0.00042	Reactome
Platelet activation, signaling and aggregation	190	64 (33.9%)	0.000442	Reactome
Wnt Signaling Pathway and Pluripotency	96	37 (38.5%)	0.000469	Wikipathways
Cell Cycle	408	123 (30.1%)	0.000484	Reactome
Amphetamine addiction - Mus musculus (mouse)	68	28 (41.8%)	0.000495	KEGG
PI3K-Akt signaling pathway - Mus musculus (mouse)	356	107 (30.7%)	0.000509	KEGG
Downregulation of SMAD2/3:SMAD4 transcriptional activity	23	13 (56.5%)	0.000546	Reactome

Supplementary Table 4: Enriched Pathway Analyses – Increased Promoter Methylation (FL/ML vs. Controls) (2/4)

Signaling by EGFR in Cancer	163	56 (34.6%)	0.000554	Reactome
Transcriptional activity of SMAD2/SMAD3:SMAD4 heterotrimer	37	18 (48.6%)	0.000577	Reactome
ErbB signaling pathway - <i>Mus musculus</i> (mouse)	87	34 (39.1%)	0.000584	KEGG
Cocaine addiction - <i>Mus musculus</i> (mouse)	50	22 (44.9%)	0.000604	KEGG
Focal adhesion - <i>Mus musculus</i> (mouse)	206	68 (33.0%)	0.000666	KEGG
DAP12 signaling	147	51 (34.9%)	0.00073	Reactome
Mitotic G2-G2/M phases	105	39 (37.1%)	0.000786	Reactome
Axon guidance - <i>Mus musculus</i> (mouse)	129	46 (35.7%)	0.000789	KEGG
Wnt signaling pathway - <i>Mus musculus</i> (mouse)	144	50 (35.0%)	0.000799	KEGG
Signaling by ERBB2	144	50 (35.0%)	0.000799	Reactome
Calcium signaling pathway - <i>Mus musculus</i> (mouse)	183	61 (33.5%)	0.000799	KEGG
Regulation of Insulin Secretion by Glucagon-like Peptide-1	40	18 (47.4%)	0.000863	Reactome
Regulation of PLK1 Activity at G2/M Transition	79	31 (39.2%)	0.000924	Reactome
MAPK signaling pathway	158	54 (34.2%)	0.000934	WikiPathways
SHC1 events in ERBB2 signaling	24	13 (54.2%)	0.000941	Reactome
Glutamatergic synapse - <i>Mus musculus</i> (mouse)	115	41 (36.3%)	0.001	KEGG
Leukocyte transendothelial migration - <i>Mus musculus</i> (mouse)	121	43 (35.8%)	0.00103	KEGG
G2/M Transition	103	38 (36.9%)	0.00106	Reactome
Integrin alphaiib beta3 signaling	27	14 (51.9%)	0.00106	Reactome
Nucleotide Metabolism	19	11 (57.9%)	0.00113	WikiPathways
Arrhythmogenic right ventricular cardiomyopathy (ARVC) - <i>Mus musculus</i> (mouse)	74	29 (39.2%)	0.00136	KEGG
Hedgehog Signaling Pathway	22	12 (54.5%)	0.00137	WikiPathways
Insulin Signaling	157	53 (33.8%)	0.00142	WikiPathways
Senescence and Autophagy	98	36 (36.7%)	0.00154	WikiPathways
Downregulation of ERBB2:ERBB3 signaling	12	8 (66.7%)	0.0016	Reactome
Generic Transcription Pathway	123	43 (35.0%)	0.0018	Reactome
p38 MAPK Signaling Pathway	34	16 (47.1%)	0.00181	WikiPathways
Glycogen Metabolism	34	16 (47.1%)	0.00181	WikiPathways
IL-6 signaling Pathway	99	36 (36.4%)	0.00189	WikiPathways
Dilated cardiomyopathy - <i>Mus musculus</i> (mouse)	90	33 (37.1%)	0.00199	KEGG
Cytoplasmic Ribosomal Proteins	79	30 (38.0%)	0.00204	WikiPathways
Hemostasis	412	120 (29.2%)	0.00205	Reactome
Post-translational protein modification	164	54 (33.1%)	0.00207	Reactome
MASTL Facilitates Mitotic Progression	10	7 (70.0%)	0.00213	Reactome
Role of DCC in regulating apoptosis	10	7 (70.0%)	0.00213	Reactome
Long-term potentiation - <i>Mus musculus</i> (mouse)	66	26 (39.4%)	0.00217	KEGG
Rap1 signalling	15	9 (60.0%)	0.00232	Reactome
Myometrial Relaxation and Contraction Pathways	157	52 (33.1%)	0.0025	WikiPathways
G alpha (z) signalling events	29	14 (48.3%)	0.00256	Reactome
Signalling to ERKs	35	16 (45.7%)	0.00262	Reactome
Adrenoceptors	8	6 (75.0%)	0.00273	Reactome
VEGF binds to VEGFR leading to receptor dimerization	8	6 (75.0%)	0.00273	Reactome
Fc epsilon receptor (FCER1) signaling	155	51 (33.1%)	0.00274	Reactome
Downstream signaling of activated FGFR	130	44 (34.1%)	0.00277	Reactome
Kit Receptor Signaling Pathway	67	26 (38.8%)	0.00278	WikiPathways
Transmission across Chemical Synapses	178	57 (32.4%)	0.00283	Reactome
NCAM signaling for neurite out-growth	55	22 (40.7%)	0.00283	Reactome
superoxide radicals degradation	4	4 (100.0%)	0.00284	MouseCyc
Adipogenesis	133	45 (33.8%)	0.00298	WikiPathways
Id Signaling Pathway	51	21 (41.2%)	0.003	WikiPathways

Supplementary Table 4: Enriched Pathway Analyses – Increased Promoter Methylation (FL/ML vs. Controls) (3/4)

Morphine addiction - <i>Mus musculus</i> (mouse)	93	33 (36.3%)	0.00301	KEGG
IL-4 signaling Pathway	61	24 (39.3%)	0.00322	Wikipathways
heparan sulfate biosynthesis (late stages)	21	11 (52.4%)	0.00331	MouseCyc
Role of LAT2/NTAL/LAB on calcium mobilization	96	34 (35.8%)	0.00336	Reactome
IL-5 Signaling Pathway	68	26 (38.2%)	0.00353	Wikipathways
Interleukin-2 signaling	39	17 (43.6%)	0.00362	Reactome
B Cell Receptor Signaling Pathway	156	51 (32.7%)	0.00369	Wikipathways
Gene Expression	720	192 (27.3%)	0.00389	Reactome
Amyotrophic lateral sclerosis (ALS) - <i>Mus musculus</i> (mouse)	52	21 (40.4%)	0.00395	KEGG
HTLV-1 infection - <i>Mus musculus</i> (mouse)	285	82 (30.1%)	0.00396	KEGG
Adaptive Immune System	457	127 (28.5%)	0.00406	Reactome
Proteoglycans in cancer - <i>Mus musculus</i> (mouse)	229	70 (30.8%)	0.00408	KEGG
Endocytosis - <i>Mus musculus</i> (mouse)	224	67 (31.0%)	0.0042	KEGG
Signaling by Wnt	49	20 (40.8%)	0.00421	Reactome
Regulation of KIT signaling	16	9 (56.2%)	0.00422	Reactome
DAP12 interactions	158	51 (32.5%)	0.00426	Reactome
TGF-beta Receptor Signaling Pathway	150	49 (32.7%)	0.00444	Wikipathways
Melanogenesis - <i>Mus musculus</i> (mouse)	100	35 (35.0%)	0.00448	KEGG
IL-2 Signaling Pathway	76	28 (36.8%)	0.00466	Wikipathways
Regulation of Apoptosis	11	7 (63.6%)	0.00469	Reactome
Mitotic M-M/G1 phases	202	63 (31.2%)	0.0047	Reactome
Fcgamma receptor (FCGR) dependent phagocytosis	66	25 (37.9%)	0.00482	Reactome
Signaling by TGF-beta Receptor Complex	66	25 (37.9%)	0.00482	Reactome
SMAD4 MH2 Domain Mutants in Cancer	66	25 (37.9%)	0.00482	Reactome
Loss of Function of SMAD4 in Cancer	66	25 (37.9%)	0.00482	Reactome
SMAD2/3 Phosphorylation Motif Mutants in Cancer	66	25 (37.9%)	0.00482	Reactome
SMAD2/3 MH2 Domain Mutants in Cancer	66	25 (37.9%)	0.00482	Reactome
Loss of Function of SMAD2/3 in Cancer	66	25 (37.9%)	0.00482	Reactome
TGFBR2 MSI Frameshift Mutants in Cancer	66	25 (37.9%)	0.00482	Reactome
TGFBR2 Kinase Domain Mutants in Cancer	66	25 (37.9%)	0.00482	Reactome
Loss of Function of TGFBR2 in Cancer	66	25 (37.9%)	0.00482	Reactome
TGFBR1 LBD Mutants in Cancer	66	25 (37.9%)	0.00482	Reactome
TGFBR1 KD Mutants in Cancer	66	25 (37.9%)	0.00482	Reactome
Loss of Function of TGFBR1 in Cancer	66	25 (37.9%)	0.00482	Reactome
Signaling by TGF-beta Receptor Complex in Cancer	66	25 (37.9%)	0.00482	Reactome
SHC1 events in ERBB4 signaling	19	10 (52.6%)	0.00485	Reactome
Circadian entrainment - <i>Mus musculus</i> (mouse)	99	34 (35.1%)	0.00491	KEGG
TNF-alpha NF-κB Signaling Pathway	184	58 (31.5%)	0.00506	Wikipathways
Chronic myeloid leukemia - <i>Mus musculus</i> (mouse)	74	27 (37.0%)	0.00508	KEGG
Regulation of Actin Cytoskeleton	151	49 (32.5%)	0.00513	Wikipathways
Regulation of actin dynamics for phagocytic cup formation	53	21 (39.6%)	0.00515	Reactome
Cyclin A/B1 associated events during G2/M transition	22	11 (50.0%)	0.00525	Reactome
Gastrin-CREB signalling pathway via PKC and MAPK	188	59 (31.4%)	0.00525	Reactome
Oxidative Stress	28	13 (46.4%)	0.00552	Wikipathways
VEGF signaling pathway - <i>Mus musculus</i> (mouse)	60	23 (38.3%)	0.00566	KEGG
DCC mediated attractive signaling	14	8 (57.1%)	0.00617	Reactome
Activation of Rac	14	8 (57.1%)	0.00617	Reactome
Signaling by NOTCH	81	29 (35.8%)	0.00642	Reactome
ADP signalling through P2Y purinoceptor 1	9	6 (66.7%)	0.00658	Reactome
Toll Like Receptor 4 (TLR4) Cascade	106	36 (34.0%)	0.00689	Reactome
FCER1 mediated MAPK activation	38	16 (42.1%)	0.00705	Reactome
Thrombin signalling through proteinase activated receptors (PARs)	17	9 (52.9%)	0.00715	Reactome

Supplementary Table 4: Enriched Pathway Analyses – Increased Promoter Methylation (FL/ML vs. Controls) (4/4)

Glucagon signaling in metabolic regulation	37	15 (42.9%)	0.00739	Reactome
RNA Polymerase I Transcription Termination	20	10 (50.0%)	0.00772	Reactome
GnRH signaling pathway - <i>Mus musculus</i> (mouse)	89	31 (34.8%)	0.00778	KEGG
GAB1 signalosome	90	31 (34.8%)	0.00778	Reactome
Signaling by FGFR1 mutants	26	12 (46.2%)	0.00803	Reactome
EPO Receptor Signaling	26	12 (46.2%)	0.00803	Wikipathways
Tight junction - <i>Mus musculus</i> (mouse)	138	44 (32.4%)	0.00818	KEGG
G alpha (12/13) signalling events	55	21 (38.2%)	0.00843	Reactome
Glycerolipid metabolism - <i>Mus musculus</i> (mouse)	56	21 (38.2%)	0.00843	KEGG
Antigen processing: Ubiquitination & Proteasome degradation	129	42 (32.6%)	0.00854	Reactome
Androgen Receptor Signaling Pathway	111	37 (33.3%)	0.00868	Wikipathways
Signaling by NOTCH1	62	23 (37.1%)	0.00893	Reactome
Signaling by NOTCH1 t(7;9)(NOTCH1:M1580_K2555) Translocation Mutant	62	23 (37.1%)	0.00893	Reactome
Signaling by NOTCH1 HD Domain Mutants in Cancer	62	23 (37.1%)	0.00893	Reactome
Signaling by NOTCH1 PEST Domain Mutants in Cancer	62	23 (37.1%)	0.00893	Reactome
Signaling by NOTCH1 HD+PEST Domain Mutants in Cancer	62	23 (37.1%)	0.00893	Reactome
FBXW7 Mutants and NOTCH1 in Cancer	62	23 (37.1%)	0.00893	Reactome
Signaling by NOTCH1 in Cancer	62	23 (37.1%)	0.00893	Reactome
AKT phosphorylates targets in the nucleus	7	5 (71.4%)	0.00899	Reactome
CREB phosphorylation	7	5 (71.4%)	0.00899	Reactome
NF-kappa B signaling pathway - <i>Mus musculus</i> (mouse)	103	33 (34.0%)	0.00915	KEGG
APC/C-mediated degradation of cell cycle proteins	39	16 (41.0%)	0.00944	Reactome
Regulation of mitotic cell cycle	39	16 (41.0%)	0.00944	Reactome
Focal Adhesion	182	56 (30.8%)	0.00994	Wikipathways

Supplementary Table 5: Enriched Pathway Analyses – Decreased Promoter Methylation (FL/ML vs. Controls) (1/3)

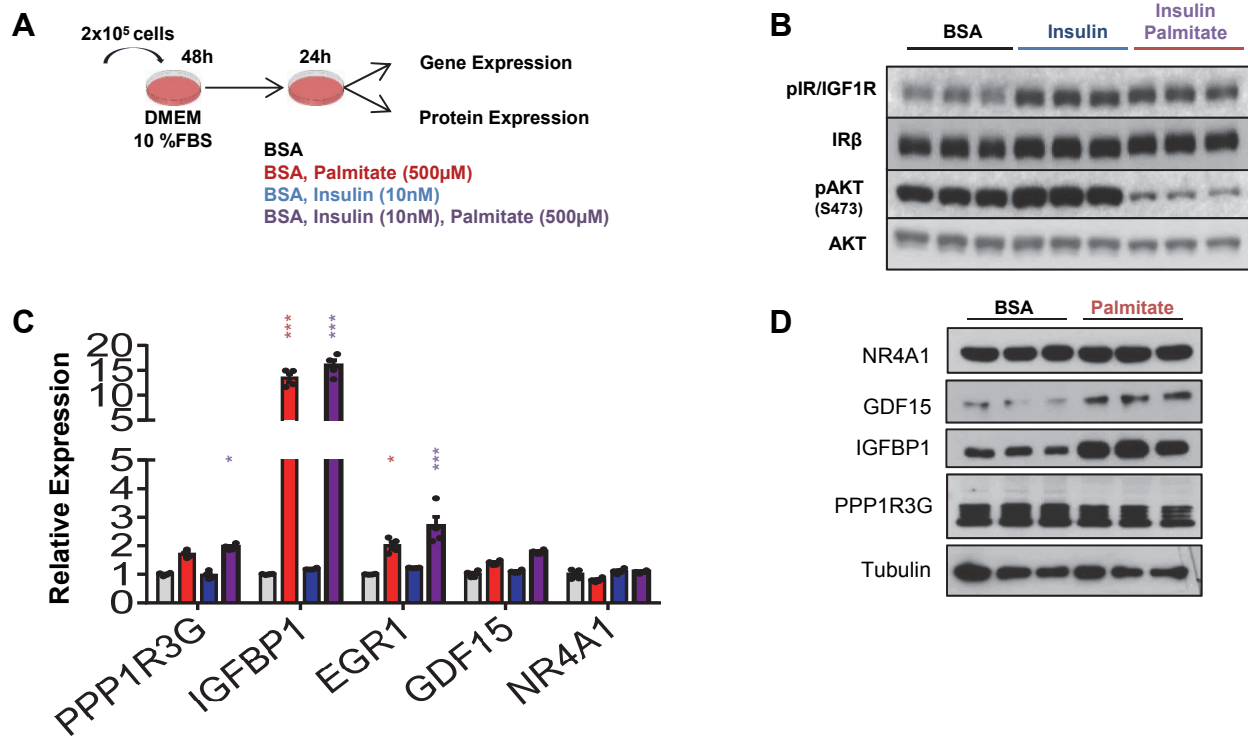
Decreased Promoter Methylation (Me.<0%; FDR<5%)	set size	candidates contained	p-value	pathway source
Wnt Signaling Pathway NetPath	109	35 (32.4%)	3.37E-06	Wikipathways
ISG15 antiviral mechanism	25	13 (52.0%)	1.52E-05	Reactome
Antiviral mechanism by IFN-stimulated genes	25	13 (52.0%)	1.52E-05	Reactome
Rho GTPase cycle	118	35 (29.7%)	2.96E-05	Reactome
Signaling by Rho GTPases	118	35 (29.7%)	2.96E-05	Reactome
p75 NTR receptor-mediated signalling	87	28 (32.2%)	3.62E-05	Reactome
XPodNet - protein-protein interactions in the podocyte expanded by STRING	831	164 (19.8%)	3.64E-05	Wikipathways
eNOS activation	9	7 (77.8%)	4.39E-05	Reactome
Hepatitis B - Mus musculus (mouse)	148	40 (27.4%)	6.23E-05	KEGG
Hippo signaling pathway - Mus musculus (mouse)	156	42 (26.9%)	6.41E-05	KEGG
G Protein Signaling Pathways	91	28 (30.8%)	8.90E-05	Wikipathways
Signalling by NGF	275	64 (23.4%)	0.000115	Reactome
eNOS activation and regulation	19	10 (52.6%)	0.000133	Reactome
Metabolism of nitric oxide	19	10 (52.6%)	0.000133	Reactome
Exercise-induced Circadian Regulation	49	18 (36.7%)	0.000135	Wikipathways
B Cell Receptor Signaling Pathway	156	41 (26.3%)	0.000139	Wikipathways
Activation of Kainate Receptors upon glutamate binding	16	9 (56.2%)	0.000149	Reactome
TNF-alpha NF-kB Signaling Pathway	184	46 (25.0%)	0.000202	Wikipathways
Membrane Trafficking	148	38 (26.2%)	0.000256	Reactome
Apoptosis	83	25 (30.1%)	0.000301	Wikipathways
Activation of Ca-permeable Kainate Receptor	11	7 (63.6%)	0.000305	Reactome
Ionotropic activity of Kainate Receptors	11	7 (63.6%)	0.000305	Reactome
Myometrial Relaxation and Contraction Pathways	157	40 (25.5%)	0.000337	Wikipathways
RIG-I/MDA5 mediated induction of IFN-alpha/beta pathways	45	16 (35.6%)	0.000482	Reactome
Pathways in cancer - Mus musculus (mouse)	326	70 (21.7%)	0.000591	KEGG
Colorectal cancer - Mus musculus (mouse)	64	20 (31.2%)	0.000699	KEGG
Pentose phosphate pathway - Mus musculus (mouse)	30	12 (40.0%)	0.000725	KEGG
Wnt signaling pathway - Mus musculus (mouse)	144	36 (25.2%)	0.000829	KEGG
Huntington's disease - Mus musculus (mouse)	189	42 (24.0%)	0.00092	KEGG
Trafficking of AMPA receptors	27	11 (40.7%)	0.001	Reactome
Glutamate Binding, Activation of AMPA Receptors and Synaptic Plasticity	27	11 (40.7%)	0.001	Reactome
Viral carcinogenesis - Mus musculus (mouse)	236	51 (22.8%)	0.00101	KEGG
Antigen Activates B Cell Receptor Leading to Generation of Second Messengers	31	12 (38.7%)	0.00102	Reactome
Pancreatic cancer - Mus musculus (mouse)	67	20 (30.3%)	0.00108	KEGG
Phosphatidylinositol signaling system - Mus musculus (mouse)	81	23 (28.4%)	0.00128	KEGG
Dopaminergic synapse - Mus musculus (mouse)	135	33 (25.2%)	0.00132	KEGG
Bacterial invasion of epithelial cells - Mus musculus (mouse)	77	22 (28.6%)	0.00147	KEGG
Apoptosis - Mus musculus (mouse)	82	23 (28.0%)	0.00153	KEGG
G-protein mediated events	45	15 (33.3%)	0.00154	Reactome
Protein processing in endoplasmic reticulum - Mus musculus (mouse)	169	40 (23.7%)	0.00159	KEGG
Oxidative Damage	17	8 (47.1%)	0.00164	Wikipathways
Toxoplasmosis - Mus musculus (mouse)	113	29 (25.7%)	0.00186	KEGG
Estrogen signaling pathway - Mus musculus (mouse)	99	26 (26.5%)	0.00189	KEGG
Lysosome Vesicle Biogenesis	23	9 (42.9%)	0.0019	Reactome
Inositol phosphate metabolism	46	15 (32.6%)	0.00197	Reactome
NRAGE signals death through JNK	46	15 (32.6%)	0.00197	Reactome
Calcium Regulation in the Cardiac Cell	150	36 (24.0%)	0.00206	Wikipathways
NOSTRIN mediated eNOS trafficking	5	4 (80.0%)	0.00216	Reactome
Cell death signalling via NRAGE, NRIF and NADE	65	19 (29.2%)	0.00227	Reactome

Supplementary Table 5: Enriched Pathway Analyses – Decreased Promoter Methylation (FL/ML vs. Controls) (2/3)

Proteoglycans in cancer - <i>Mus musculus</i> (mouse)	229	50 (22.0%)	0.00238	KEGG
Recruitment of NuMA to mitotic centrosomes	11	6 (54.5%)	0.00255	Reactome
Apoptosis Modulation by HSP70	18	8 (44.4%)	0.00258	WikiPathways
EGFR interacts with phospholipase C-gamma	34	12 (35.3%)	0.00259	Reactome
mRNA Processing	163	38 (23.3%)	0.00273	Reactome
ZBP1(DAI) mediated induction of type I IFNs	31	11 (36.7%)	0.00274	Reactome
Opioid Signalling	66	19 (28.8%)	0.00275	Reactome
Cellular Senescence	111	28 (25.2%)	0.0029	Reactome
Cytosolic sensors of pathogen-associated DNA	58	17 (29.8%)	0.003	Reactome
Intrinsic Pathway for Apoptosis	39	13 (33.3%)	0.00311	Reactome
Diurnally Regulated Genes with Circadian Orthologs	48	15 (31.2%)	0.00315	WikiPathways
PodNet- protein-protein interactions in the podocyte	315	65 (20.6%)	0.00326	WikiPathways
glutathione biosynthesis	3	3 (100.0%)	0.0033	MouseCyc
PLCG1 events in ERBB2 signaling	35	12 (34.3%)	0.00341	Reactome
Glycogen breakdown (glycogenolysis)	15	7 (46.7%)	0.00344	Reactome
PLC beta mediated events	44	14 (31.8%)	0.00355	Reactome
Glutathione and one carbon metabolism	31	11 (35.5%)	0.00369	WikiPathways
Glutathione metabolism	19	8 (42.1%)	0.00387	WikiPathways
Synthesis of IP3 and IP4 in the cytosol	27	10 (37.0%)	0.0039	Reactome
One carbon metabolism and related pathways	49	15 (30.6%)	0.00392	WikiPathways
Regulation of actin cytoskeleton - <i>Mus musculus</i> (mouse)	218	47 (21.8%)	0.00406	KEGG
Phospholipase C-mediated cascade	54	16 (29.6%)	0.00422	Reactome
Tetrahydrobiopterin (BH4) synthesis, recycling, salvage and regulation	12	6 (50.0%)	0.00445	Reactome
Primary Focal Segmental Glomerulosclerosis FSGS	71	19 (27.5%)	0.00473	WikiPathways
DAG and IP3 signaling	32	11 (34.4%)	0.00487	Reactome
Neuronal System	254	53 (21.0%)	0.005	Reactome
Gene Expression	720	129 (18.3%)	0.00537	Reactome
Elevation of cytosolic Ca2+ levels	9	5 (55.6%)	0.00544	Reactome
Small cell lung cancer - <i>Mus musculus</i> (mouse)	86	22 (25.9%)	0.00561	KEGG
Glutathione synthesis and recycling	6	4 (66.7%)	0.00572	Reactome
Cam-PDE 1 activation	6	4 (66.7%)	0.00572	Reactome
Cellular responses to stress	127	30 (23.6%)	0.00593	Reactome
Apoptosis	101	25 (24.8%)	0.00613	Reactome
Processing of Capped Intron-Containing Pre-mRNA	144	33 (22.9%)	0.00658	Reactome
mRNA Splicing - Major Pathway	112	27 (24.1%)	0.00659	Reactome
mRNA Splicing	112	27 (24.1%)	0.00659	Reactome
PluriNetWork	291	59 (20.3%)	0.00672	WikiPathways
Alzheimer's disease - <i>Mus musculus</i> (mouse)	181	37 (22.3%)	0.00673	KEGG
FAS pathway and Stress induction of HSP regulation	38	12 (31.6%)	0.00721	WikiPathways
TRAF3-dependent IRF activation pathway	13	6 (46.2%)	0.00724	Reactome
DARPP-32 events	25	9 (36.0%)	0.00755	Reactome
Synaptic vesicle cycle - <i>Mus musculus</i> (mouse)	62	17 (27.4%)	0.00765	KEGG
mTOR signaling pathway - <i>Mus musculus</i> (mouse)	62	17 (27.4%)	0.00765	KEGG
Regulation of Actin Cytoskeleton	151	34 (22.5%)	0.00778	WikiPathways
TRAF6 mediated IRF7 activation	17	7 (41.2%)	0.00792	Reactome
Laminin interactions	21	8 (38.1%)	0.00792	Reactome
PLC-gamma1 signalling	34	11 (32.4%)	0.00814	Reactome
Integrin-mediated Cell Adhesion	98	24 (24.5%)	0.00821	WikiPathways
TNF signaling pathway - <i>Mus musculus</i> (mouse)	111	26 (23.9%)	0.00874	KEGG
MicroRNAs in Cardiomyocyte Hypertrophy	83	21 (25.3%)	0.00882	WikiPathways

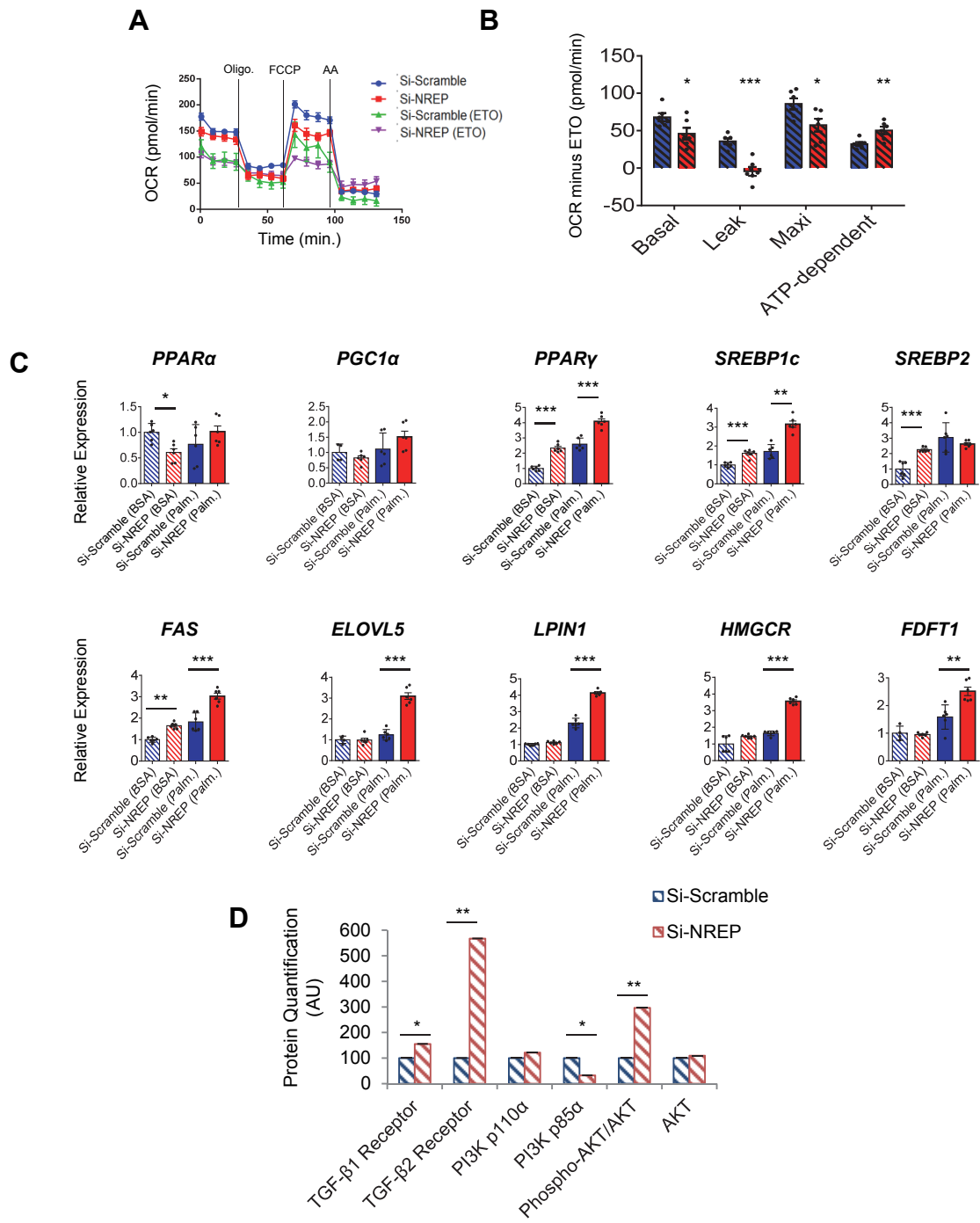
Supplementary Table 5: Enriched Pathway Analyses – Decreased Promoter Methylation (FL/ML vs. Controls) (3/3)

Hepatitis C - <i>Mus musculus</i> (mouse)	136	31 (22.8%)	0.00895	KEGG
Clathrin derived vesicle budding	61	16 (27.6%)	0.00895	Reactome
trans-Golgi Network Vesicle Budding	61	16 (27.6%)	0.00895	Reactome
Spliceosome - <i>Mus musculus</i> (mouse)	137	30 (22.9%)	0.00936	KEGG
ESC Pluripotency Pathways	110	26 (23.6%)	0.00987	Wikipathways
TRIF-mediated TLR3/TLR4 signaling	89	22 (24.7%)	0.00991	Reactome
MyD88-independent cascade	89	22 (24.7%)	0.00991	Reactome
Toll Like Receptor 3 (TLR3) Cascade	89	22 (24.7%)	0.00991	Reactome



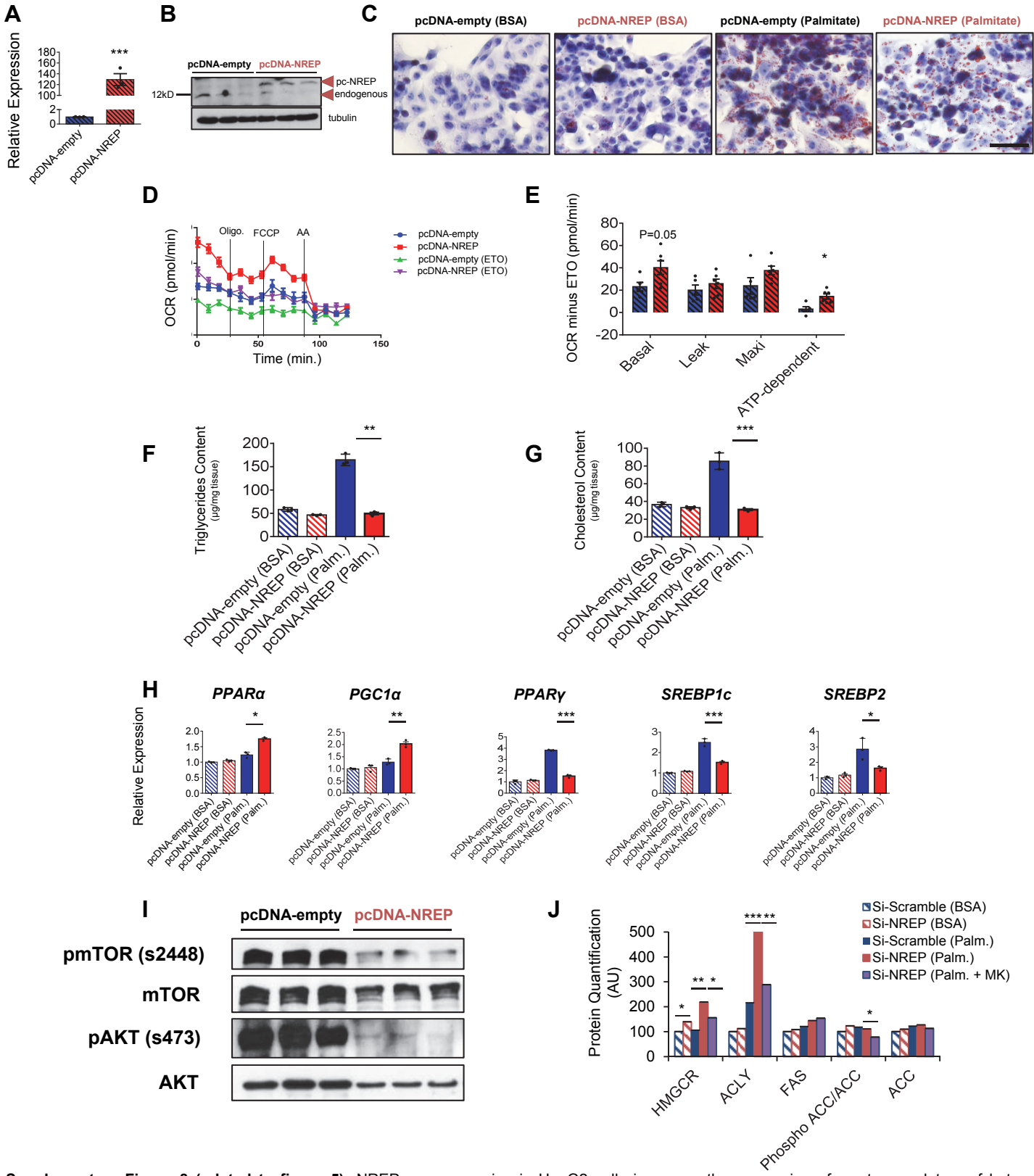
Supplementary Figure 6 (related to figure 5): (A) Schematic for the *in-vitro* modulation of hepatic steatosis. (B) Signaling analysis of lysates from HepG2 cells treated with insulin (blue) or insulin+palmitate, (purple). (C) qPCR analyses of candidate genes in cells challenged with BSA (black), palmitate (red), insulin (blue) or insulin+palmitate (purple). Insert shows values for *IGFBP1* on a higher scale. (D) Protein analyses of candidate genes in lysates from HepG2 cells challenged with BSA or palmitate. All data are based on 3 independent experiments (n=3). Statistical analyses in C by two-way ANOVA with LSD test. *P<0.05, **P< 0.01 and ***P<0.001. Data are expressed as means ± SEM.

Supplementary Figure 6 (related to Figure 5)



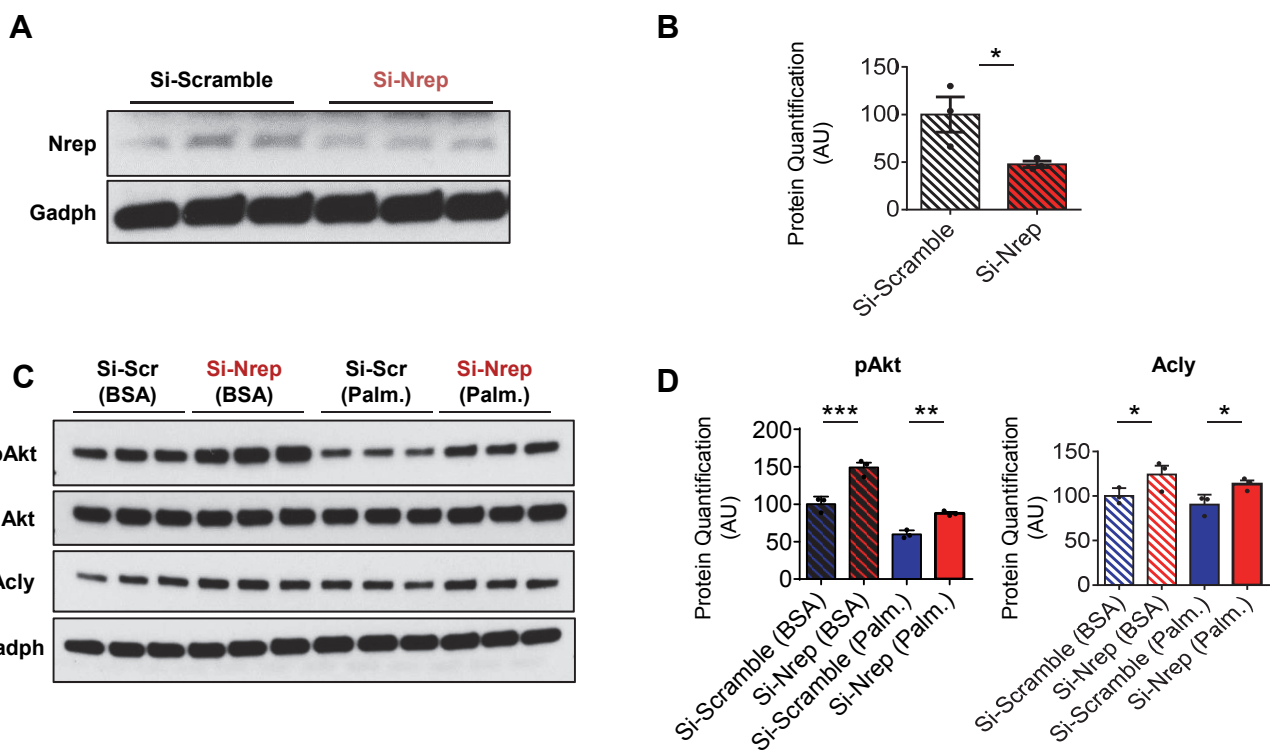
Supplementary Figure 7 (related to figure 5) **(A)** Oxygen-consumption ratio (OCR) from seahorse analyses of fatty-acid oxidation (FAO) in scramble and NREP KD treated with a BSA:palmitate substrate (n=6 experiments). **(B)** Quantification of seahorse results. **(C)** RT-PCR analyses of genes involved in β-oxidation (*PPARα*), mitochondrial biogenesis (*PGC1α*), transcriptional regulation of fatty-acid (*PPARγ*, *SREBP1c*), and cholesterol metabolism transcriptional regulation (*SREBP2*), *de-novo* fatty-acid synthesis (*FAS*), fatty-acid elongation (*ELOVL5*), glycerolipid synthesis (*LPIN1*), and cholesterol synthesis (*HMGCR*, *FDFT1*) in HepG2-scramble or NREP KD challenged with BSA or Palmitate for 24h (n=3 independent experiments). **(D)** Protein quantification of indicated proteins related to Figure 5J. Statistical analyses using One-way ANOVA with the Dunnett's post hoc test. Data are expressed as means ± SEM.

Supplementary Figure 7 (related to Figure 5)

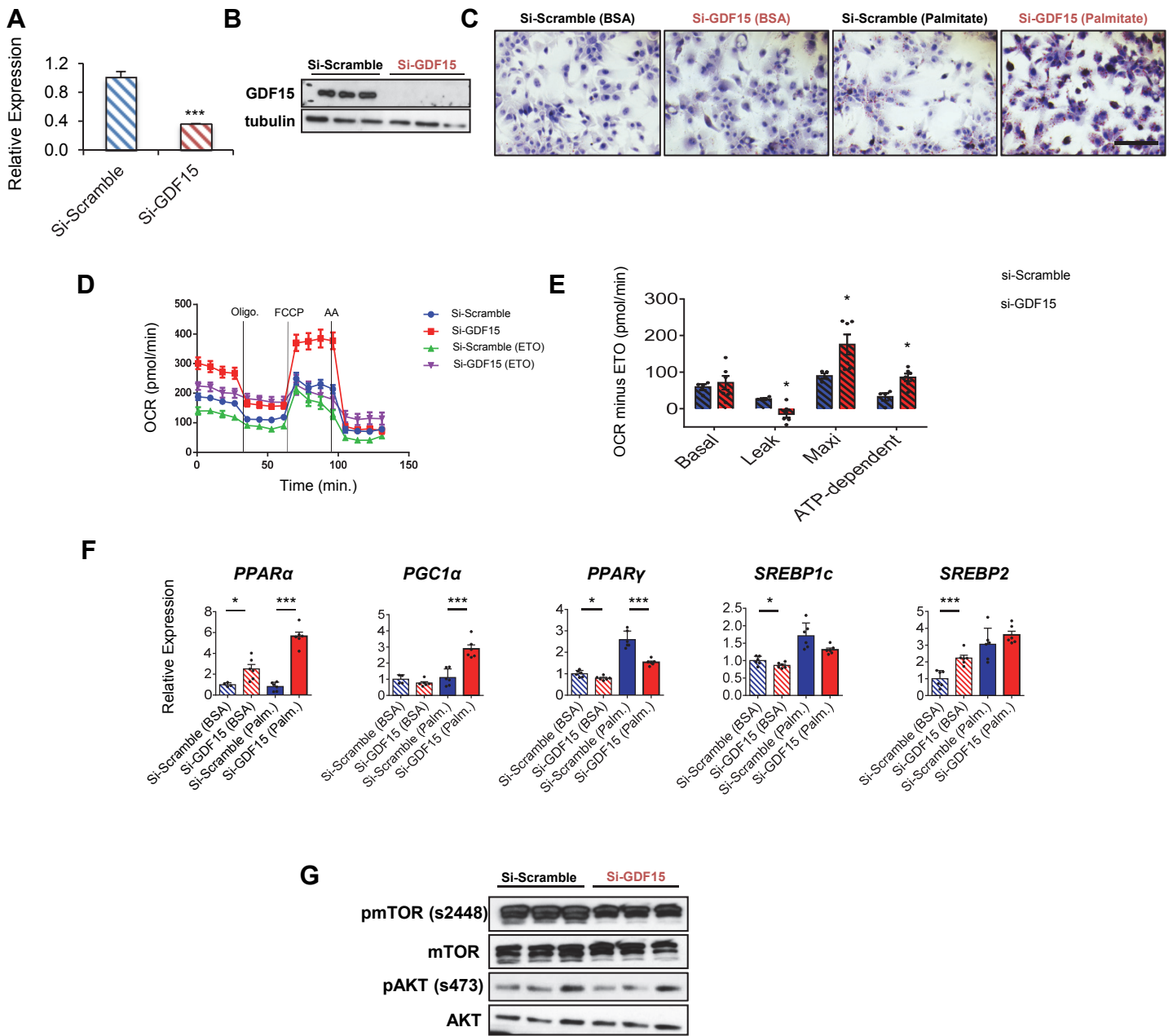


Supplementary Figure 8 (related to figure 5): NREP overexpression in HepG2 cells increases the expression of master regulators of beta-oxidation, mitochondrial biogenesis and dramatically blocks the increment of fatty-acid synthesis-related genes in response to palmitate. **(A-B)** HepG2 cells with NREP overexpression (OE) evaluated by qPCR (**A**) or western blot (**B**). **(C)** Representative oil-red staining in NREP OE HepG2 cells challenged with palmitate for 24h (magnification 400x, Scale bar = 50μm). **(D-E)** Fatty-acid oxidation (FAO) analysis by Seahorse (**D**) and quantification (**E**) in NREP OE HepG2 cells. **(F-G)** Triglycerides (**F**) and cholesterol (**G**) content quantification in lysates from HepG2 cells stimulated for 24h with 500μM of Palmitate. **(H)** qPCR analyses of genes involved in beta-oxidation, mitochondrial biogenesis and fatty-acid synthesis in HepG2 cells (scramble or NREP OE) challenged with BSA or Palmitate for 24h. **(I)** Basal signaling analyses in lysates from HepG2 cells (scramble or NREP OE). **(J)** Protein quantification of indicated proteins related to Figure 5K. All data are based on 3 independent experiments (n=3). Statistical analyses using One-way ANOVA with the Dunnett's post hoc test. . *P<0.05, **P<0.01 and ***P<0.001. Data are expressed as means ± SEM.

Supplementary Figure 8 (related to Figure 5)

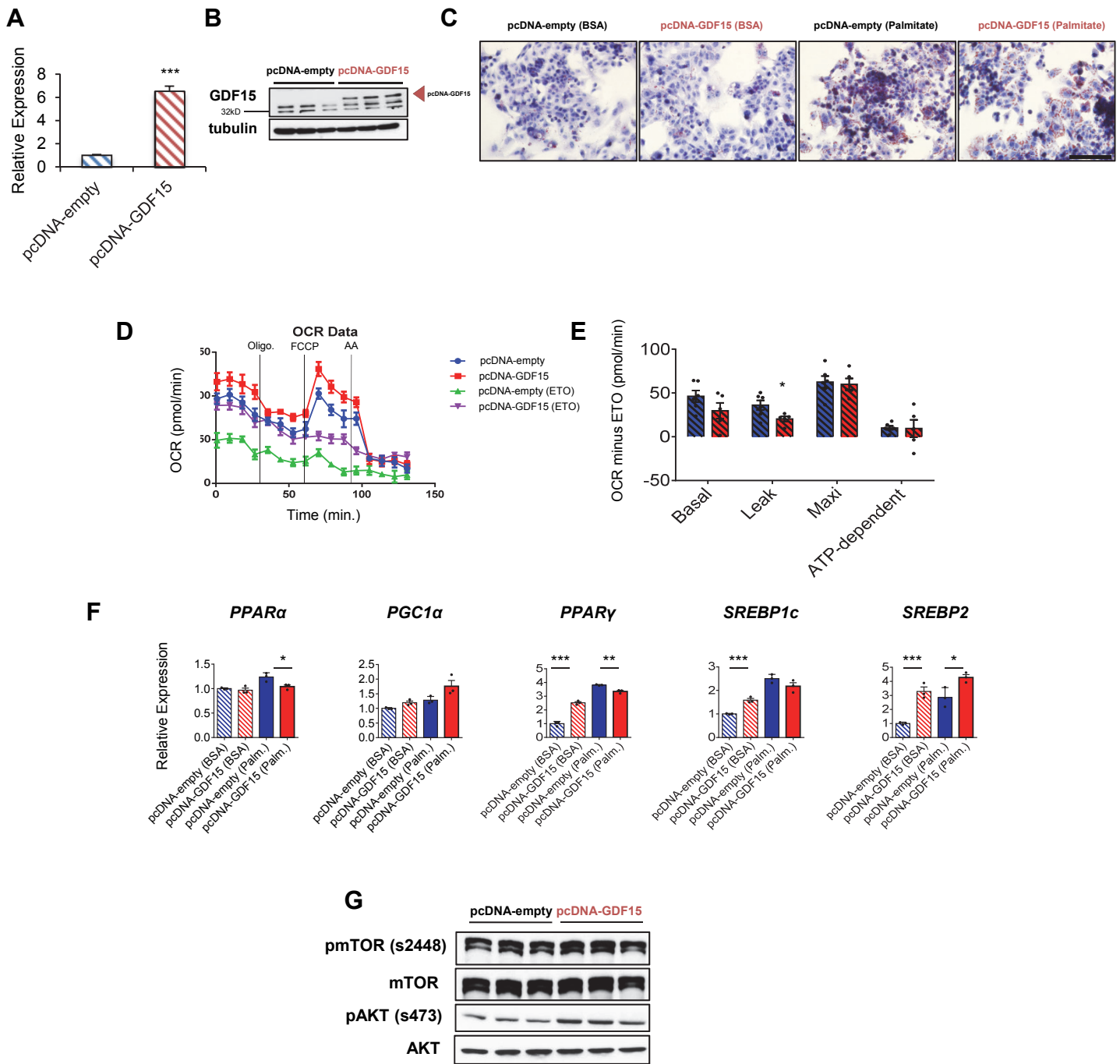


Supplementary Figure 9 (related to figure 5): NREP knock-down in AML12 cells increases phospho-Akt and ATP-citrate lyase levels. (A) Nrep knock-down (KD) in AML12 cells (n=3 independent experiments). **(B)** Quantification of indicated protein. **(C)** Protein analyses of indicated proteins in AML12 cells Scramble or Nrep KD treated with BSA or palmitate for 24h (n=3 independent experiments/group). **(D)** Quantification of indicated proteins. Statistical analyses using unpaired two-tailed t-test in B and one-way ANOVA with Fisher's LSD test in D. * P<0.05, ** P<0.01 and ***P<0.001. Data are expressed as means ± SEM.



Supplementary Figure 10 (related to figure 5): GDF15 modulates the expression of genes involved in mitochondrial biogenesis, beta-oxidation and fatty-acid metabolism. GDF15 knockdown (KD) in HepG2 cells evaluated by (A) qPCR or (B) protein levels. (C) Representative oil-red staining in HepG2 cells challenged with BSA or Palmitate for 24h (magnification 400x, Scale bar = 50μm). (D-E) Fatty-acid oxidation (FAO) analysis by seahorse (D) and quantification (E) in HepG2 cells with KD of GDF15. (F) qPCR analyses of genes involved in beta-oxidation, mitochondrial biogenesis and fatty-acid synthesis in HepG2-scramble or GDF15 KD challenged with BSA or Palmitate for 24h. GDF15 overexpression (OE) in HepG2 cells evaluated by (G) qPCR or (G) protein levels. All data are based on 3 independent experiments (n=3) and 2-group comparisons analyzed using an unpaired two-tailed Student's t-test. *P<0.05, ** P< 0.01 and ***P< 0.001. Data are expressed as means ± SEM.

Supplementary Figure 10 (related to Figure 5)



Supplementary Figure 11 (related to figure 5): GDF15 modulates the expression of genes involved in mitochondrial biogenesis, beta-oxidation and fatty-acid metabolism. GDF15 knockdown (KD) in HepG2 cells evaluated by (A) qPCR or (B) protein levels. (C) Representative oil-red staining in HepG2 cells challenged with BSA or Palmitate for 24h (magnification 400x, Scale bar = 50μm). (D-E) Fatty-acid oxidation (FAO) analysis by seahorse (D) and quantification (E) in HepG2 cells with KD of GDF15. (F) qPCR analyses of genes involved in beta-oxidation, mitochondrial biogenesis and fatty-acid synthesis in HepG2-scramble or GDF15 KD challenged with BSA or Palmitate for 24h. GDF15 overexpression (OE) in HepG2 cells evaluated by (G) qPCR or (G) protein levels. All data are based on 3 independent experiments (n=3) and 2-group comparisons analyzed using an unpaired two-tailed Student's t-test. *P<0.05, **P< 0.01 and ***P< 0.001. Data are expressed as means ± SEM.

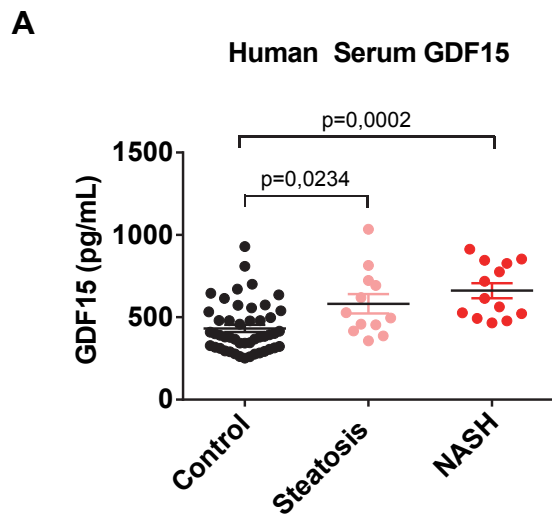
Supplementary Figure 11 (related to Figure 5)

Supplementary Table 6: Patient information of human liver samples

Xenotech ID	Group	% Macro Fat	AGE	Gender	Ethnicity	BMI	Alcohol Use
H1299	Control 1	0	17	F	Caucasian	20.6	Occasional
H1283	Control 2	0	64	F	Caucasian	29.1	Occasional
H1336	Control 3	0	60	F	African American	24.1	Occasional
H1262	Control 4	0	26	M	Caucasian	22.9	Occasional
H1290	Control 5	0	51	M	Hispanic	30	Occasional
H1307	Control 6	0	50	M	Asian	26.4	No
H1288	Control 7	0	59	F	Caucasian	31.4	Occasional
H1235	Steatosis 1	30-40	38	M	Caucasian	31.9	Occasional
H1237	Steatosis 2	20	58	M	Caucasian	32.09	Occasional
H1243	Steatosis 3	75	41	M	Caucasian	23.5	Heavy
H1278	Steatosis 4	20	41	M	Caucasian	32	No
H0820	Steatosis 5	60	65	F	Caucasian	49.9	No
H0851	Steatosis 6	50	47	F	Caucasian	47.4	No
H1082	Steatosis 7	40	66	F	Caucasian	24	No
H0818	Steatosis 8	40	48	M	Hispanic	32.5	No

Supplementary Table 7: Clinical characteristics of the Kuopio Obesity Surgery (KOBS) study

Kuopio Obesity Surgery (KOBS) study		n=170
Male/Female		37/133
Age (years)		48.06 ± 9.23
BMI		41.80 ± 4.59
Glucose (mmol/l)		6.07 ± 1.42
Insulin (pmol/l)		113.04 ± 65.73
Cholesterol (mmol/l)		4.29 ± 0.91
HDL cholesterol (mmol/l)		1.21 ± 0.31
LDL cholesterol (mmol/l)		2.47 ± 0.82
Triglycerides (mmol/l)		1.39 ± 0.69
Type 2 diabetes (%)		22.35 %
Histology (normal / simple steatosis / NASH)		106/36/28

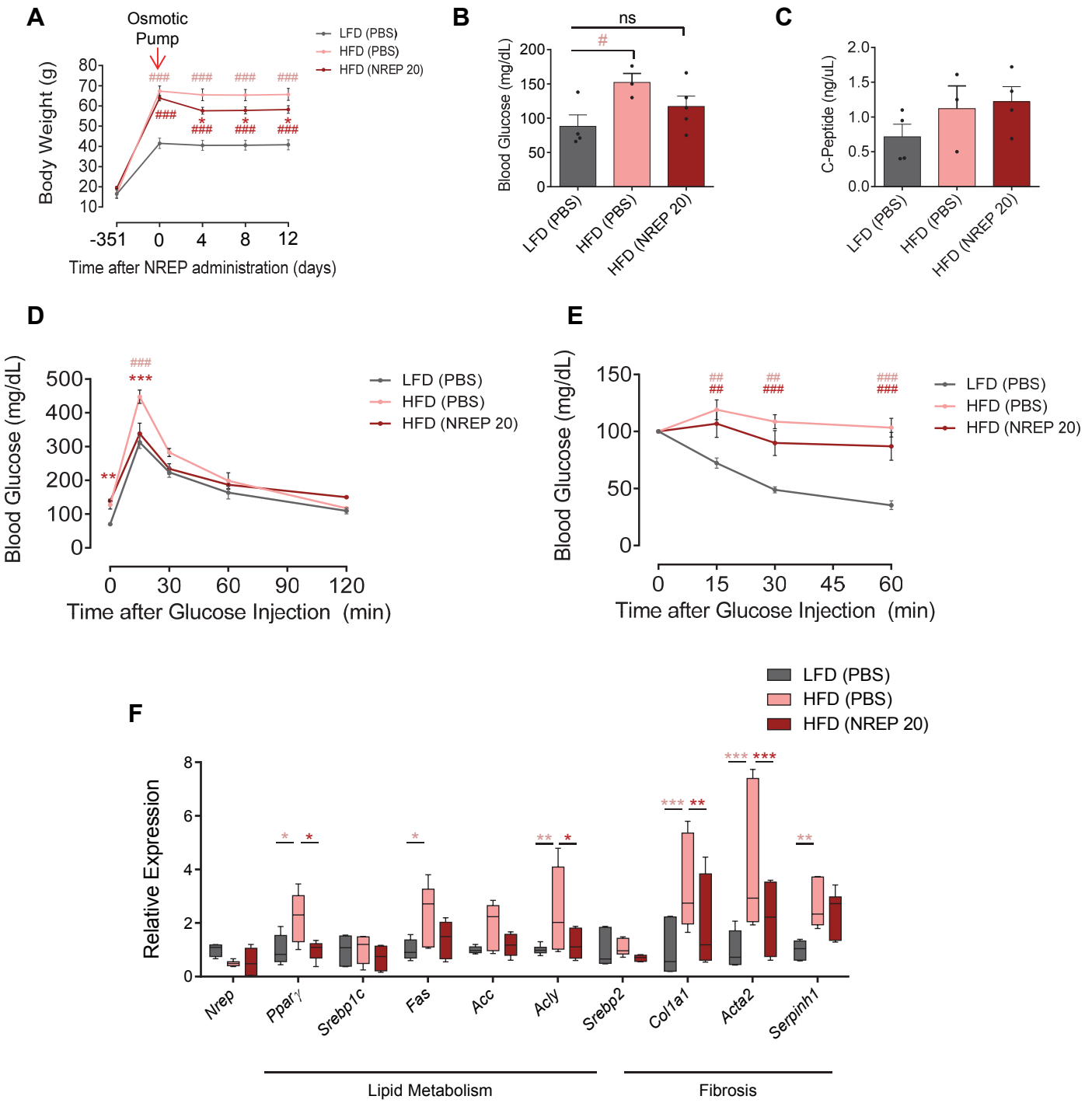


B

n=75		Correlation	Adj. Sex, age & BMI	Adj. Sex, age, BMI & T2D
HDL-C	rho	0.107	-0.036	0.010
	p value	0.369	0.765	0.932
Triglycerides	rho	0.193	0.245	0.175
	p value	0.104	0.042	0.153
Fasting Insulin	rho	0.293	0.441	0.371
	p value	0.012	1.4E-04	0.002
Steatosis grade	rho	0.548	0.700	0.649
	p value	3.7E-07	7.6E-12	9.1E-10
Lobular inflammation	rho	0.463	0.546	0.500
	p value	2.9E-05	7.0E-07	8.9E-06
NAS (NAFLD Activity Score)	rho	0.552	0.692	0.637
	p value	2.8E-07	1.7E-11	2.4E-09



Supplementary Figure 12 (related to figure 7): GDF15 plasma levels in NAFLD patients. (A) GDF15 plasma levels in obese control, steatosis and NASH patients (Control, n=48; Steatosis, n=12; NASH, n=13). (B) Plasma GDF15 correlations with clinical parameters. (C) ROC curves of GDF15 in controls versus steatosis plus NASH. Significance was determined by one-way ANOVA with Kruskal-Wallis test with Dunn's multi comparisons test in A. Adjusted spearman correlations in B. Data are expressed as means \pm SEM. *P< 0.05, **P< 0.01 and ***P< 0.001.



Supplementary Figure 13 (related to figure 7): Human recombinant NREP administration by an osmotic pump improves glucose control, and hepatic lipid and fibrotic gene expression profile in long-term HFD fed mice. (A) Body weigh trajectories (LFD-PBS, n=4 independent biological samples; HFD-PBS, n=3 independent biological samples; HFD-NREP 20, n=5 independent biological samples). LFD-PBS received PBS 0.1% BSA, HFD-PBS received PBA 0.1% BSA and HFD-NREP20 received human recombinant NREP diluted in PBSA 0.1% BSA. (B) 5-hour fasted blood glucose levels 12 days after osmotic pumps implementation (LFD-PBS, n=4 independent biological samples; HFD-PBS, n=3 independent biological samples; HFD-NREP 20, n=5 independent biological samples). (C) 5-hour fasted C-peptide levels 12 days after osmotic pumps implementation (LFD-PBS, n=4 independent biological samples; HFD-PBS, n=3 independent biological samples; HFD-NREP 20, n=5 independent biological samples). (D) Blood glucose excursions after a glucose intraperitoneal challenge 12 days after osmotic pumps implementation (LFD-PBS, n=4 independent biological samples; HFD-PBS, n=3 independent biological samples; HFD-NREP 20, n=5 independent biological samples). (E) Blood glucose excursions after an insulin intraperitoneal challenge 12 days after osmotic pumps implementation (LFD-PBS, n=4 independent biological samples; HFD-PBS, n=3 independent biological samples; HFD-NREP 20, n=5 independent biological samples). (F) Hepatic RT-PCR gene expression analyses of indicated genes (LFD-PBS, n=3 independent biological samples; HFD-PBS, n=3 independent biological samples; HFD-NREP 20, n=3 independent biological samples performed in technical replicates). Relative expression to *Tbp*. Data are expressed as means \pm SEM. Statistical analyses by one-way ANOVA with Dunnett's multiple comparisons test in (A-C); two-way ANOVA Dunnett's multiple comparisons test in (D-E) and two-way ANOVA with Fisher's LSD test in F. In A-D * represent statistical comparisons between HFD-PBS versus HFD-NREP20 and # represent statistical comparisons between HFD-PBS or HFD-NREP20 to LFD-PBS. *or # P<0.05, ** or ## P<0.01, and *** or ### P<0.001.

Supplementary Table 8: RT-qPCR primers
1/2

Mouse Primers RT-PCR	Forward	Reverse
<i>β-actin</i>	CGTAAAAGATGCCAGATCA	CACAGCCTGGATGGCTACGT
<i>Ppara</i>	GTACCACTACGGAGTTCACGCAT	CGCCGAAAGAAGCCCTTAC
<i>Pgc1a</i>	GAGAATGAGGCAAACCTGCTAGCG	TGCATGGTCTGAGTGCTAAGACC
<i>Ppary</i>	TGGCCACCTCTTGCTCTGCTC	AGGCCGAGAAGGAGAAGCTGTTG
<i>Srebp1c</i>	ACGACGGAGCCATGGATTGCAC	CCGGAAGGCAGGCTTGAGTACC
<i>Fas</i>	TGCAACTGTGCGTTAGCCACC	TGTTTCAGGGAGAGAGAGACC
<i>Acc</i>	GACAGACTGATCGCAGAGAAAG	TGGAGAGCCCCACACACA
<i>Glut2</i>	GGCTAATTCAAGGACTGGTT	TTTCTTGCCCTGACTTCCT
<i>Pepck1</i>	GTGGGAGTGACACCTCACAGC	AGGACAGGGCTGGCGGGAGC
<i>mG6pd</i>	ATGAACATTCTCCATGACTTTGGG	GACAGGAACTGTTTATTATAGG
<i>Aldob</i>	AGCCTCTGAGAAGGATGCTC	GTCCAGCATGAAGCAGTTGAC
<i>Gys</i>	ACTGCTGGCGTTATCTCTGTG	ATGCCCGCTCCATGCGTA
<i>C/EBPα</i>	TGGACAAGAACAGCAACGAG	TCACTGGTCAACTCCAGCAC
<i>Scd1</i>	AGATCTCCAGTTCTACACGACCAC	GTGGACCTTCTCTGTAGGCAG
<i>ChREBP</i>	CTGGGGACCTAACAGGAGC	GAAGCCACCCCTATAGCTCCC
<i>aP2</i>	CACCGCAGACGACAGGAAG	GCACCTGCACCAGGGC
<i>Mcp1</i>	AGCACCAGCCAACCTCTCAC	TCTGGACCCATTCTCTTGTG
<i>Nrep</i>	GGTGTGGTACTTTGTTCTGG	CTCACACTCTTGGTAGCATCCAC
<i>Nmrk1</i>	AGAGCTTGAGAACGACCTTCC	CATCCAAACAGGAAACTGCTGACA
<i>Vhl</i>	GTTTGTGCCATCCCTCAATGTCG	ACCTGACGATGTCCAGTCTCCT
<i>Ankrd9</i>	GCAGTGGCTTACACCATTGGAG	TCCTCAGACGAAGTGGTGTGG
<i>Homer2</i>	TCCAGGAGGTAAAGAGAACGCTGC	GTCTGTGCCATTGACGCTGGAT
<i>Ppp1r3g</i>	CTTCACGGAGTGGCGTACCTT	AGGCACACCGAGTGGAAAC
<i>Igfbp1</i>	GCCCAACAGAAAGCAGGAGATG	GTAGACACACCAGCAGAGTCCA
<i>Egr1</i>	AGCGAACAAACCTATGAGCACC	ATGGGAGGCACCGAGTCGTTT
<i>Gdf15</i>	AGCCGAGAGGACTCGAACCTCAG	GGTTGACCGCGAGTAGCAGCT
<i>Nr4a1</i>	GTGCAGTCTGGTGACAATGC	CAGGCAGATGTACTGGCGCTT
<i>Syne1</i>	CAGCCATTCACTGTGAGCAGCT	CACCATCCAGACCTTAAGGCT
<i>Cpeb2</i>	GAGATCACTGCCAGCTCCGAA	CAATGAGTGCCTGGACTGAGCT
<i>Trib3</i>	CTGCGTCGCTTGTCTTCAGCA	CTGAGTATCTGGTCCCACGT
<i>Spon2</i>	CGACAGTGGTTCACCTCTCC	AGGACTTGAGGCAGGGTAGTA
<i>Serpine1</i>	CCTCTCCACAAGTCTGATGGC	GCAGTTCCACAACGTCTACTCG
<i>Frmd4b</i>	CAGTTCATGGACACCAGGCATTC	TGCTGTAGGCATTCCGAGTCAG

Supplementary Table 8: RT-qPCR primers
2/2

Human Primers RT-PCR	Forward	Reverse
<i>β-ACTIN</i>	CACCATTGGCAATGAGCGGTTC	AGGTCTTGCAGATGCCACGT
<i>NREP</i>	TCCAAACAAGGACATGGAGGG	AGGTAACTGATTCTGGGGAG
<i>PPP1R3G</i>	GGATGCCAAGAAAGAGCCAGGC	GGTAGCAGACAGCGAAGTGGAC
<i>IGFBP1</i>	TCCTTGGACGCCATCAGTAC	GATGTCTCTGTGCCCTGGCTA
<i>EGR1</i>	AGCAGCACCTCAACCCCTCAGG	GAGTGGTTGGCTGGGTAAC
<i>GDF15</i>	GGCCAACCAGAGCTGGGAAG	GCCCAGAGAGATAACCGAGGTG
<i>NR4A1</i>	GGACAACGCTTCATGCCAGCAT	CCTTGTTAGCCAGGCAGATGTAC
<i>PPARα</i>	TCCTGAGCCATGCAGAATTAC	AGTCTAAGGCCTCGCTGGTG
<i>PGC1</i>	CCAAAGGATGCGCTCTGTTCA	CGGTGTCTGTAGTGGCTTGACT
<i>PPARγ</i>	AGCCTGCGAAAGCCTTTGGTG	GGCTTCACATTCAAGCAAACCTGG
<i>SREBP1c</i>	CTCCGGCCACAAGGTACACA	GAGGCCCTAACGGTTGACACAG
<i>SREBP2</i>	CGGGCGCAACGCAAAC	AATTGCAGCATCTCGTCGATGT
<i>FAS</i>	TTCTACGGCTCCACGCTCTCC	GAAGAGTCTCGAGGGCTAGCAATG
<i>ELOVL5</i>	GAGCGTTCTGTGCTGCG	CTAGTATCTGAGGGCTAGCAATG
<i>LPIN1</i>	TGCCAGTGTAGTCCAGACAGCA	GAGGTCATCCAAGTAGACGC
<i>HMGCR</i>	TTCGGTGGCCTCTAGTGAGA	TGTCACTGCTCAAAACATCCTCT
<i>FDFT1</i>	GACTCGACAGACTCTAAGGCTC	TGGTCAATAAGTCGCCACG

Supplementary Table 9: Reagents information

Antibodies		
Anti-NREP (IHC-P)	Abcam	167017
Anti-NREP (WB)	Thermo Fisher	PA5-68426
Anti-Phospho-AKT	Cell Signaling	9271
Anti-AKT	Cell Signaling	9272
Anti-Phospho-GSK3β	Cell Signaling	5536
Anti-GSK3β	Cell Signaling	12456
Anti-Phospho-mTOR	Cell Signaling	5536
Anti-mTOR	Cell Signaling	2983
Anti-HMGCR	Abcam	214018
Anti-Phospho-IR/IGF1R	Cell Signaling	3021
Anti-IRβ	Cell Signaling	3025
Anti-NR4A1	Cell Signaling	3960
Anti-GDF15	Cell Signaling	8479
Anti-IGFBP1	Abcam	181141
Anti-PPP1R3G	Abcam	11275
Anti-ATP-citrate lyase	Cell Signaling	13390
Anti-αTUBULIN	Abcam	7291
Anti-βACTIN	Cell Signaling	12262
Critical Commercial Assays		
High Capacity cDNA reverse transcription kit	Applied Biosystems	4368813
RNeasy Kit	Qiagen	74106
iTaq Universal SYBR Green Supermix	Applied Biosystems	4387406
Stanbio™ LiquiColor™ Enzymatic Triglycerides Test	Fisher	SB2200225
Stanbio™ LiquiColor™ Enzymatic Cholesterol Test	Fisher	SB1010225
Mouse Insulin ELISA Kit	Crystal Chem.	90080
Genta Puregene Tissue Kit	Qlagen	158667
Human NREP ELISA Kit	MyBiosource	MBS9323406
Human GDF15 ELISA Kit	R&D Systems	DGD150
Experimental Models: Organisms/Strains		
C57BL/6J DIO mice	380050	Jackson Laboratories
C57BL/6J DIO Control mice	380056	Jackson Laboratories
B6.Cg-Lepob/J mice	632	Jackson Laboratories
BKS.Cg-Dock7m +/- Leprdb/J mice	642	Jackson Laboratories
LIRKO mice	C. Ronald Kahn lab	N/A
Human Plateable Hepatocytes, 5-Donor	Fisher	HMCPP5
Recombinant DNA		
P311(NREP) Human Tagged ORF Clone	Origene	RC209945
GDF15 Human Tagged ORF Clone	Origene	RC201295
siRNAs		
siGENOME Non-Targeting siRNA #1	Dharmacon	D-001210-01-05
SMARTpool: siGENOME NREP siRNA	Dharmacon	M-019848-00-0005
SMARTpool: siGENOME GDF15 siRNA	Dharmacon	M-019875-01-0005
SMARTpool: siGENOME Nrep siRNA	Dharmacon	M-040972-01-0005

Supplemental Methods

Mice and Diets

Liver-specific insulin receptor KO mice – LIRKO (insulin receptor-IRlox/lox; Albumin-Cre+/-) mice were generated as previously described (14). In brief, the control offspring group consisted of F1 offspring from a control male and female (insulin receptor-IRlox/lox; Albumin-Cre-/-). Control parents were crossed for 4 generations to minimize any epigenetic memory from the presence of Cre. Father LIRKO offspring (FL) resulted from the crossing of a male LIRKO (insulin receptor-IRlox/lox; Albumin-Cre+/-) with a control female. Mother LIRKO offspring (ML) resulted from the breeding of a control male with a LIRKO female. The animals were matched for age (8-9 weeks) and the determination of the pregnancy day was made according to the presence of a copulation plug (vaginal plug). After confirmation of pregnancy day, the females were separated from males and single-caged. Litter sizes were normalized to 4-5 pups. Litters with less than 4 pups were excluded and litters with more than 5 pups, pups were randomly selected for sacrifice. We used only virgin females, and F1 offspring from different groups were weaned together and maintained in the same rack to minimize any microbiome effects. Since phenotypes between male and female offspring were similar (please see Fig1 and S3), we focused on the male offspring to minimize any confounding effects of female hormones. Mice were maintained on a chow diet (PicoLab® mouse diet 20 – 5058) or weaned at 3 weeks of age on a high-fat diet containing 60% fat (D12492 - Research diets Inc., USA) until 3 months of age. We purchased 12 week old male C57BL/6 mice from Jackson laboratories, and fed them on a low-fat diet (10% fat) or a 60% high-fat diet since 6 weeks of age. We also purchased control male ob+/+,db+, and the obesogenic models C57BL/6 Lep-/- and Lepr-/- at 12 weeks of age. Mice were anesthetized using Avertin and blood was collected by heart puncture from all the animals used in our experiments unless specified otherwise. Serum Insulin, C-peptide, leptin, resistin, GIP and MCP-1 were measured using the Luminex xMAP® technology (Luminex Corp.) according to manufacturer guidelines. Sample sizes for animal experiments were chosen on the basis of experience in previous in-house studies of metabolic phenotypes and to balance the ability to detect significant differences with minimization of the number of animals used in accordance with NIH guidelines.

RNA-sequencing

High quality RNA was isolated as described above and the final elution was performed in 20 µl of RNase-free sterile distilled water. The concentration and integrity of the extracted total RNA were estimated using the Qubit® 2.0 Fluorometer (Invitrogen) and Agilent 2100 Bioanalyzer (Applied Biosystems, USA), respectively. Five hundred nanograms of total RNA was required for downstream RNA-seq applications. Polyadenylated RNAs were isolated using NEBNext Magnetic Oligo d(T)25 Beads. Next, the first-strand synthesis was performed using NEBNext RNA first-strand synthesis module (New England BioLabs Inc., USA). Immediately, directional second strand synthesis was performed using NEBNExt Ultra Directional second strand synthesis kit. The NEBNext® DNA Library Prep Master Mix Set for Illumina® was then used to prepare individually bar-coded next-generation sequencing expression libraries as per the manufacturer's recommended protocol. Library quality was assessed using the Qubit 2.0 Fluorometer, and the library concentration was estimated by utilizing a DNA 1000 Chip on an Agilent 2100 Bioanalyzer. Accurate quantification for sequencing applications was determined using the qPCR-based KAPA Biosystems Library Quantification Kit (Kapa Biosystems, Inc., USA). Paired-end sequencing (100bp) was performed on an Illumina HiSeq2500 sequencer to obtain approximately 50 million reads per sample. Raw reads were de-multiplexed using bcl2fastq Conversion Software (Illumina, Inc.) with default settings.

Supplemental Methods

Enhanced Reduced Representation Bisulphite Sequencing (ERRBS)

High molecular weight DNA was isolated from control, FL and ML offspring livers using the Gentra puregene tissue kit (Qiagen) according to the manufacturer protocol. ERRBS library preparation, sequencing and post-processing of the raw data was performed at the Epigenomics Core at Weill Cornell. Briefly, 75 ng of DNA (>20kb in size) were digested with Mspl. After phenol extraction and ethanol precipitation, Mspl ends were end-repaired, A-tailed and ligated to methylated TruSeq adapters (Illumina Inc. San Diego, CA). Samples were size selected in a 1.5% agarose gel and two size fragment lengths of 150–250 bp and 250–400 bp were gel isolated. The two fractions were subjected to overnight bisulfite conversion (55 cycles of 95°C for 30 seconds, 50 °C for 15 minutes) using EZ DNA methylation kit (Zymo Research, Irvine CA). Purified bisulfate converted DNA was PCR amplified using TruSeq primers (Illumina Inc. San Diego, CA) for 18 cycles of denaturing, annealing and extension/elongation steps: 94°C for 20 seconds, 65°C for 30 seconds, 72°C for 1 minutes, followed by 72°C for 3 minutes. The resulting libraries were normalized to 2nM and pooled at the same molar ratio. The final samples were pooled according to the desired plexity, clustered at 6.5pM on single-read flow cell and sequenced for 50 cycles on an Illumina HiSeq 2500. Primary processing of sequencing images was done using Illumina's Real-Time Analysis software (RTA) as suggested by the Illumina. Illumina's BCL2FASTQ software (v2.17) was then used to de-multiplex samples and generate raw reads and respective quality scores. For analysis of bisulfite-treated sequence reads (with an average bisulfite conversion rate of >99% for all samples), reads were filtered for adapter sequences using the FLEXBAR software. Adapter sequence present in the 3' end of the reads was removed if it aligned with the adapter sequence by at least 6 bps and had at most a 0.2 mismatch error rate. Reads were aligned to the whole genome using the Bismark alignment software with a maximum of two mismatches in a directional manner and only uniquely aligning reads were retained. In order to call a methylation score for a base position, read bases aligning to that position had at least a 20 phred quality score and that base position had at least 10x coverage. The percentage of bisulfite converted cytosines (representing unmethylated cytosines) and non-converted cytosines (representing methylated cytosines) were recorded for each cytosine position in CpG, CHG, and CHH contexts (with H corresponding to A, C, or T nucleotides).

Comprehensive Laboratory Animal Monitoring System (CLAMS)

The OxyMax CLAMS system from Columbus Instruments was used to provide a direct measurement of volumetric oxygen consumption (VO₂) and carbon dioxide (CO₂) production, respiratory exchange ratio (RER), food and drinking behavior, and activity level. Measurements were obtained during 24h at dark and light cycles and a fed state. Mice were housed individually in 12 chambers and were placed into individual acclimation chambers prior to the experiment. Sampling of the chambers occurred serially completing 1 cycle every 15 minutes and was controlled by OxyMax v5.02 software. The total body weight of each mouse was entered into the system at setup and the system was calibrated using a certified O₂/CO₂ gas mixture. Drierite was replaced prior to each run to eliminate moisture from the system and maintain a constant humidity. Data analysis was provided by CLAX v2.2.10 software.

Supplemental Methods

Dual Energy X-Ray Absorptiometry (DEXA)

The DEXA system uses X-ray absorbance to assess lean and fat mass composition, bone mineral density and bone length on mice up to 55 grams in weight. We used the Lunar Piximus II densitometer (GE Lunarcorp.) DEXA system includes the scanner and software for display, analysis and database handling of images. Prior to a scanning session, the system was calibrated using a Phantom of known absorbance for fat and bone. Mice were anesthetized by 2% isoflurane inhalation administered using the EZ-1500 Isoflurane Anesthesia Machine (Euthanax Corporation PA, USA). Each mouse was initially placed in a priming chamber to induce anesthesia then moved to a nose cone for maintenance. Mice were placed on a Piximus scanning tray on the imaging platform prior to imaging. Mice were returned to their cages and monitored until emergence. Analyses of total and percent lean and fat mass were measured for total body and defined regions of interest.

Osmotic Pumps

After 351 days feeding with 10% low-fat (LFD) or a 60% high-fat (HFD) diet, osmotic pumps (Alzet 1002) carrying 100 µl of either PBS BSA (0.1%) or human recombinant NREP (NBP2-2328, Novus Biologicals, USA) diluted in PBS BSA (0.1%) at 20 ng/day/mouse were implanted subcutaneously and administered for 12 days.

Histology analyses

Mouse liver sections were fixed in 10% buffered formalin for 1h, paraffin-embedded, sectioned and stained with hematoxylin and eosin according to standard methods. HepG2 cells and human primary hepatocytes were fixed with 10% buffered formalin for 30 minutes and stained in filtered Oil Red-O for 10 minutes. Sections were washed in distilled water, counterstained with hematoxylin for 2 minutes and visualized on a microscope. For NREP immunohistochemistry, human liver sections from controls and patients with steatosis were purchased from Xenotech Inc. (Supplementary Table 5). Formalin-fixed paraffin-embedded human liver sections were processed by standard immunohistochemistry protocol. After blocking endogenous peroxidase and biotin, 5% donkey serum was used to block non-specific protein binding. Anti-P311 (NREP) antibody (Abcam #167017) was applied and incubated at 4°C overnight. Biotinylated conjugated antibody was used followed by streptavidin-peroxidase. Staining was completed by DAB chromogen.